To The Graduate School:

The members of the Committee approve the thesis of Kyle S. Cheesbrough presented on November 13, 2007.

Glenn A. Tootle, Chairman

Greg Kerr

Steven Prager

Ramesh Sivanpillai

APPROVED:

David M. Bagley, Head, Department of Civil and Architectural Engineering

Don A. Roth, Dean, The Graduate School

Cheesbrough, Kyle S., Glacial Recession in Wyoming's Wind River Range, M.S.,
Department of Civil and Architectural Engineering, December 2007

Abstract

The Wind River Range (WRR), located in western Wyoming, is host to more than 60 glaciers making it the largest concentration of glaciers in the Rocky Mountain region. Several studies have been performed on the glaciers of the WRR, dating back to the 1930's focusing on only the largest, most accessible glaciers such as Gannett and Dinwoody Glaciers. Each of the previous studies have documented the WRR glaciers as being in an overall receding trend since 1850, with some localized periods of advancement (Pochop et al., 1990).

This study documents glacial surface area change, volume change and change in terminus position for 42 glacial complexes in the WRR from 1985 through 2005, through utilization of remote sensing techniques. The use of remote sensing techniques allows more of the glaciers in the WRR to be analyzed, rather than focusing on only the most geographically accessible glaciers. In addition to documenting the area changes since 1985 for all of the WRR glaciers, the changes in surface area and terminus position for nine selected glaciers was estimated from 1966 through 2001 using aerial photographs.

It has been noted in previous studies that glaciers of smaller area are typically more sensitive to changes in climate than large glaciers (Granshaw & Fountain, 2006). Out of the 42 glacial complexes analyzed, 25 of them had an area of <0.5 km^2 in 1985, while the others were >0.5 km^2 in 1985. The glaciers that had <0.5 km^2 surface area in 1985 experienced an average percent loss of 43%, while the large glaciers (>0.5 km^2) experienced an average decrease of 28%. In addition to reductions in size, it was found that WRR glaciers make appreciable contributions to downstream flows.

Glacial Recession in Wyoming's Wind River Range

by

Kyle S. Cheesbrough

A thesis submitted to the Department of Civil and Architectural Engineering
and the Graduate School of the University of Wyoming
in partial fulfillment of the requirements
for the degree of

MASTER OF SCIENCE
in
CIVIL ENGINEERING

Laramie, Wyoming
December, 2007

UMI Number: 1449779

Table of Contents

1.0 Introduction 1

1.1 Glaciers of the Western United States 1

1.2 Glaciers of the Wind River Range, Wyoming, USA 2

1.3 Dinwoody Glacier 3

1.4 Research Objectives 4

2.0 Study Area 6

2.1 Wind River Range, Wyoming 6

2.2 Dinwoody Glacier 9

3.0 Data and Methods 10

3.1 Area analysis using Landsat satellite imagery (1985 to 2005) for 42 glacial complexes ... 12

3.2 Volume analysis for 42 glacial complexes 14

3.3 Area analysis using Aerial Photography (1966-2001) for six glacial complexes 14

3.4 Stereo analysis of USGS aerial photos for Dinwoody Glacier 17

3.5 Field Data collected from Dinwoody Glacier 18

4.0 Results 23

4.1 Glacial area change for 42 glacial complexes from 1985 to 2005 23

4.2 Glacial volume change for 42 glacial complexes from 1985 to 2005 27

4.3 Glacial area change for six glacial complexes from 1966 to 2001 31

4.4 Glacial area change for Dinwoody Glacier 33

4.5 Analysis of field data 37

4.5.1 Ice-Depth Data 37

4.5.2 Repeat Terrestrial Photography 39

5.0 Conclusions 42

6.0 Acknowledgements 44

7.0 References 45

8.0 Appendices 48

8.1 Appendix 1: Personnel and Equipment / Supplies used for 2006 Fieldwork 48

8.2 Appendix 2: Locations of GPS Point Measurements 49

8.3 Appendix 3: Locations of Radar Depth Measurements 51

8.4 Appendix 4: Comparison of GPS & Stereo Model Elevations 53

List of Tables

Table 1: Wind River Glacial Complexes Studied 8

Table 2: Information Regarding Sattelite Images Used for Area Change Analysis. 12

Table 3: Information Regarding Aerial Photographs Used for Area Change Analysis... 15

Table 4: Aerial Photographs Used to Document Dinwoody Glacier Volume Change.... 17

Table 5: Changes in Surface Area for 42 Glacial Complexes 24

Table 6: Volume Changes for 42 Glacial Complexes. 28

Table 7: Percent Contibution of Glacier Runoff to Streamflow. 31

Table 8: Changes in Surface Area for Secondary Glacial Network 32

Table 9: Differences in Surface Area as Calculated via Landsat and Aerial Photos....... 33

List of Figures

Figure 1: Glaciated Regions of the Western United States.. 1

Figure 2: Location Map of the Wind River Range. 7

Figure 3: Description of Datasets used for Analysis. 11

Figure 4: Location of GPS Elevation Readings 20

Figure 5: Location of Radar Ice Depth Readings 21

Figure 6: Change in Glacier Surface Area for 42 Glacial Complexes............................ 25

Figure 7: Spatial Variations in Surface Area Changes for 42 Glacial Complexes 26

Figure 8: Spatial Variations in Volume Change for 42 Glacial Complexes.................... 29

Figure 9: Location Map of Watersheds that have Glacial Contributions 30

Figure 10: Change in Surface Area for six Glacial Complexes (1966-2001)................. 32

Figure 11: Changes in Terminus Position for Dinwoody Glacier (1966-2001) 34

Figure 12: Topographic Map of Dinwoody Glacier (2001)... 35

Figure 13: Three-Dimensional Image of Dinwoody Glacier (1983). 36

Figure 14: Three-Dimensional Image of Dinwoody Glacier (2001). 36

Figure 15: Ice Depth Comparisons of Dinwoody Glacier (1988 & 2006) 38

Figure 16: Repeat Ground Photographs of Dinwoody Glacier (1935, 1988 & 2006)..... 40

Figure 17: Repeat Ground Photographs of Dinwoody Glacier (1935, 1988 & 2006)..... 41

1.0 Introduction

1.1 Glaciers of the Western United States

There are approximately 1,100 glaciers in the conterminous United States (lower 48 states), with an approximate surface area of 530 square kilometers (km^2). The majority of the glaciers in the conterminous U.S. occur in western states including, Washington, Wyoming, Montana, Oregon, California, Colorado and Idaho (Figure 1) (Meier and Post, 1962, Fountain, 2006).

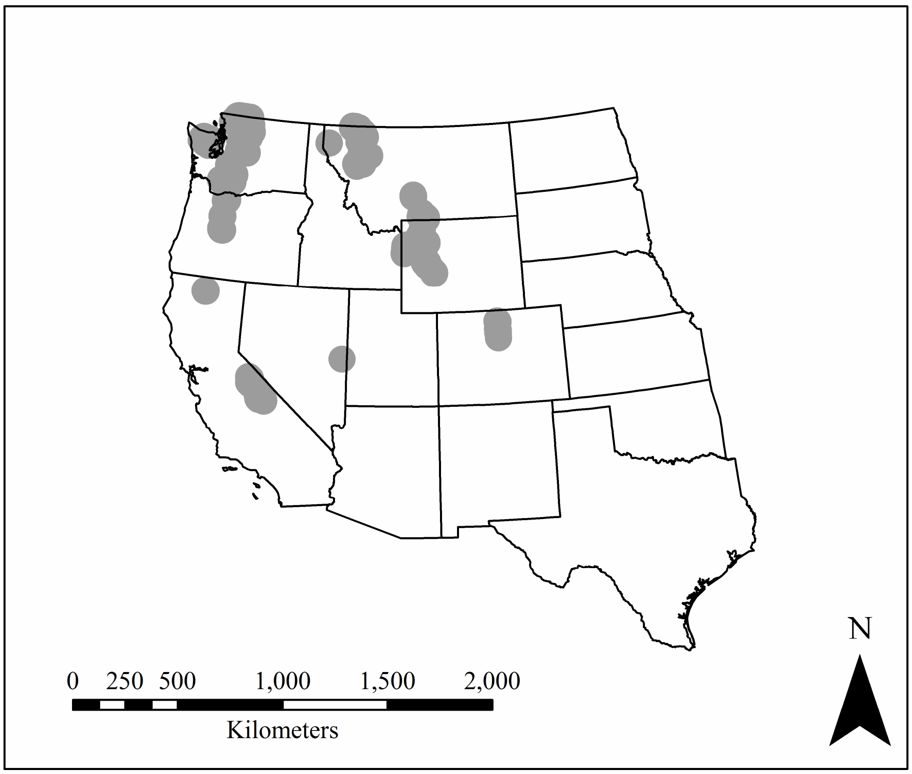

Figure 1: Glaciated regions of the Western United States (from Fountain, 2006).

The glaciers of the western U.S. greatly influence the development of water resources in the region. Glacially populated watersheds are shown to provide a more stable water source than non-glaciated basins (Ferguson, 1973, Fountain and Tangborn 1985, Braithwaite and Olsen, 1988). Glaciated watersheds have approximately 50%

greater summer runoff and less runoff variability than non-glaciated basins (Fountain and Tangborn, 1985).

Many major rivers originate from glaciers and the downstream flow characteristics of glaciers make them valuable for mid to late summer water supply needs. Glaciers typically reach their maximum discharge rates in late summer, while downstream domestic and agricultural needs are highest.

1.2 Glaciers of the Wind River Range, Wyoming, USA

Wyoming is host to approximately 80 glaciers, with a surface area of approximately 47 km^2 (Meier, 1969). The Wind River Range contains 63 glaciers, making it the largest concentration of glaciers in the American Rocky Mountains. Although glaciers are found along the entire length of the Wind River Range, the highest concentration of glaciers is found in the northern portion of the range, with the largest glaciers also occurring in the northern portion of the range (Meier, 1951). The vast majority of glaciers occur at the higher elevations near the continental divide. Gannett and Dinwoody glaciers, two of the largest glaciers in the American Rocky Mountains, are located at approximately 43.175°N, 109.65°W. It is common belief that the glaciers of the Wind River Range are a result of ‘The Little Ice Age’ ending in 1850 (Marston et al. 2001). ‘The Little Ice Age’ is a documented cool period starting circa 1745 and ending in 1850, that was preceded by a warm period from 1650 to 1745 (Naftz, 2002).

The glaciers of the Wind River Range have been the subject of several studies, dating back to the 1930’s, although reports of glacier existence in Wyoming’s Wind River Range date back to the 1870’s. Meier (1951) performed one of the first detailed inventories of glaciers in the Wind River Range. This study included detailed descriptions, elevation-area relationships, extensive photography and maps for more than 20 glaciers.

Several authors (e.g., Meier, 1951; Dyson 1953; Mears 1972) have noted that the glaciers of the Wind River Range have been in a receding state since the end of the Little Ice Age (circa 1850), with several localized periods of advancement. Love and Thompson (1987, 1988) showed evidence that many of the glaciers of the Wind River Range had re-advanced to their original (1850) position by 1930, which may be supported by a documented cool period between 1915 and 1930 (Naftz 2002).

1.3 Dinwoody Glacier

Dinwoody is a relatively accessible glacier in the Wind River Range, thus it has been studied rigorously in previous research efforts, including Meier (1951), Marston et al. (1991) and Wolken (2000). The 1951 study by Meier estimated the surface area of Dinwoody Glacier to be 3.47 km^2. Meier and Post (1962) later estimated that the surface area of Dinwoody Glacier had decreased to 3.44 km^2. Marston et al. (1991) performed the next in-depth study of Dinwoody and Gannett Glaciers estimating the area of Dinwoody Glacier to be 2.91 km^2. The Marston et al. (1991) study also utilized aerial photograph stereopairs from 1958 and 1983 to obtain elevation measurements on the glaciers. By comparing the difference in elevation for the two different dates, volume change estimates were obtained. Marston et al. also estimated that Dinwoody glacier had lost 64×10^6 m^3 of water equivalent from 1958 to 1983 and the measured ice depths of Dinwoody Glacier ranged between 54 and 111m. In addition to estimating volume change, the remaining volume of ice for Dinwoody Glacier was estimated using radio-echo sounding measurements collected on the glacier.

Wolken (2000) followed the Marston et al. (1991) study by mapping the perimeter of Dinwoody Glacier in 1999. Points along the perimeter of the glacier were recorded using a GPS and mapped in a Geographical Information System (GIS) to calculate the updated surface area of Dinwoody Glacier. A topographic survey was also conducted by Wolken (2000) to determine surface elevations of Dinwoody glacier. In 1999 the surface area of Dinwoody Glacier was calculated to be 2.19 km^2 (Wolken, 2000).

An updated volume change was also estimated by Wolken (2000) by comparing elevation information from the 1983 stereopairs done by Marston et al. (1991) to stereopairs from 1994. The volume lost from 1983 to 1994 was calculated to be 43×10^6 m^3 for the 11-year period (Wolken, 2000).

1.4 Research Objectives

The current research utilizes remote sensing data and techniques to quantify glacier area changes for 42 glacial complexes in Wyoming's Wind River Range from 1985 to 2005. The results from the area analysis were utilized in area-volume scaling techniques to estimate glacier volume changes from 1985 to 2005. Next, six of the 42 glacial complexes were analyzed using aerial photographs to determine area change. The use of aerial photographs resulted in extending the period of record back to 1966 (1966 to 2001). Finally, aerial photograph stereopairs have been analyzed to gain topographical information for the surface of Dinwoody Glacier. The results from the stereopair analysis of Dinwoody Glacier provided volume change estimates by comparing changes in the surface elevations over time. The results of the stereopair analysis of Dinwoody Glacier were compared to the previous results which applied area-volume scaling techniques.

Additionally, field data collected from Dinwoody Glacier in August, 2006 were compared to both the area-volume scaling techniques and stereopair analysis results for verification purposes. The results from each of the above tasks provided a means for estimating glacial meltwater contributions to streamflows in the region.

2.0 Study Area

2.1 Wind River Range, Wyoming

The Wind River Range in Wyoming is an unbroken 180 km mountain range that extends from west-central Wyoming to northwestern Wyoming (Pochop et al., 1990). The highest elevations of the Wind River Range form part of the Continental Divide, which also acts as the boundary between Fremont and Sublette Counties in Wyoming (Figure 2 and Table 1).

The Wind River Range serves as the headwaters for both the Colorado and the Missouri Rivers. The Green River begins in the northern Wind River Mountain range and flows south before reaching the confluence of the Colorado River. The Wind River flows from the east slope of the Wind River range before becoming the Bighorn River, which flows north until the confluence with the Yellowstone River which then confluences with the Missouri River. Many of the creeks and streams that serve the Green and Wind/Bighorn Rivers are glacial fed.

Seven of the ten largest glaciers in the Rocky Mountain region are located in the Wind River Range (Pochop et al., 1990), near Gannett Peak, the highest point in Wyoming (elevation 4,207 m). The main concentration of glaciers in the Wind River Range can be accessed from either the east or west side of the range. From the east slope, the glaciers are accessed via an approximately 40 km hike on the Glacier Trail. Access is limited to non-mechanized travel since the area is mainly wilderness. This route serves as an access to the termini of Dinwoody and Gannett Glaciers.

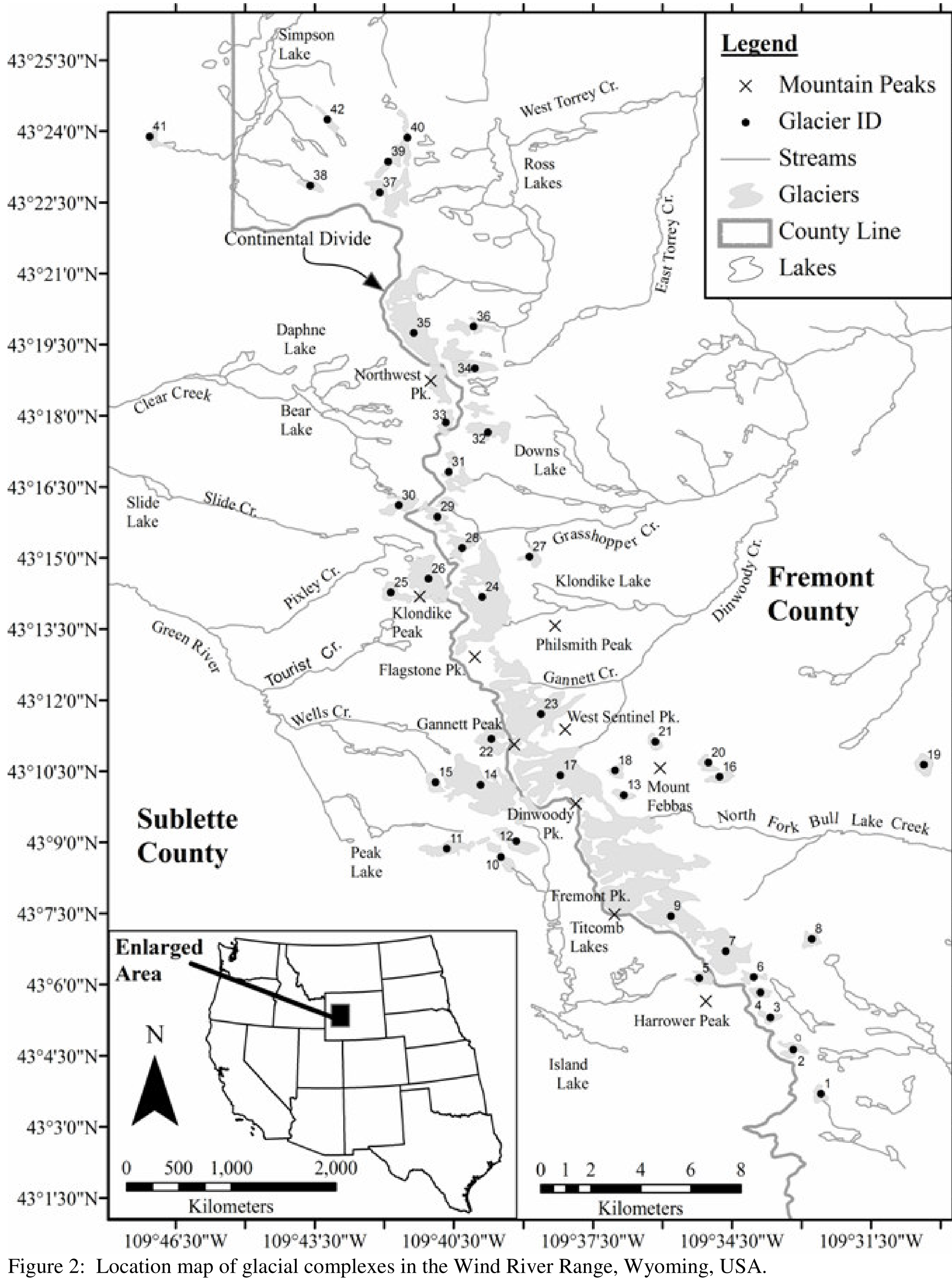

Figure 2: Location map of glacial complexes in the Wind River Range, Wyoming, USA.

Table 1: Wind River Range glacial complexes (ID, name, latitude, longitude and aspect) identified for current research (NN denotes an unnamed glacial complex).

Site ID	Glacier Names	Latitude	Longitude	Aspect
1	NN	43.06161	-109.54304	East
2	NN	43.07713	-109.55295	East
3	NN	43.08842	-109.56125	East
4	NN	43.09724	-109.56479	East
5	Harrower Glacier	43.10225	-109.58681	West
6	NN	43.10265	-109.56718	East
7	Knife Point Glacier	43.1117	-109.57726	East
8	NN	43.11603	-109.54629	East
9	Bull Lake Glacier	43.12408	-109.59697	East
	Upper Fremont Glacier			East
	Sacagawea Glacier			East
	Helen Glacier			East
10	NN	43.14481	-109.65802	West
11	Stroud Glacier	43.14781	-109.67756	West
12	Twins Glacier	43.15044	-109.65259	West
	NN			West
13	NN	43.16663	-109.61389	East
14	Mammoth Glacier	43.17023	-109.66542	West
15	Baby Glacier	43.17111	-109.6816	West
16	NN	43.17303	-109.57949	East
17	Dinwoody Glacier	43.17354	-109.63677	East
	NN			East
18	Heap Steep Glacier	43.17527	-109.61706	East
19	NN	43.17726	-109.50609	East
20	NN	43.17805	-109.58353	East
21	NN	43.18542	-109.6026	East
22	Minor Glacier	43.18638	-109.66152	West

Site ID	Glacier Names	Latitude	Longitude	Aspect
23	Gannett Glacier	43.19511	-109.64365	East
	Gooseneck Glacier			East
	NN			East
24	Grasshopper Glacier	43.23628	-109.66481	East
25	J Glacier	43.23786	-109.69766	West
26	Sourdough Glacier	43.24272	-109.68415	West
27	NN	43.25042	-109.64783	East
28	NN	43.25349	-109.67199	East
29	NN	43.26447	-109.68096	East
	NN			East
30	Connie Glacier	43.26854	-109.69483	West
31	NN	43.28026	-109.67685	East
32	Downs Glacier	43.29414	-109.66278	East
	NN			East
	NN			East
33	NN	43.29758	-109.67791	West
34	NN	43.31668	-109.66748	East
	NN			East
35	Continental Glacier	43.3291	-109.68942	East
	NN			East
	NN			West
36	NN	43.33142	-109.66796	East
37	NN	43.37849	-109.70163	East
38	NN	43.38092	-109.72662	East
39	NN	43.38937	-109.69866	East
40	NN	43.39779	-109.69169	East
41	NN	43.39814	-109.78432	West
42	NN	43.40416	-109.72046	East

2.2 Dinwoody Glacier

Ground truth measurements were taken on Dinwoody Glacier in August, 2006. Dinwoody Glacier is located southeast of Gannett Peak and is the most accessible of the Wind River Range glaciers. Dinwoody Glacier is composed of three steep, cirque-type ice masses and a single large lobe that makes up the main body of the glacier. The higher elevations of Dinwoody Glacier are extremely steep, often over 45 degrees, as well as very crevassed, making it difficult to access the upper portions. The elevations of Dinwoody Glacier range from about 3,400 m to over 4,000 m (Meier, 1951).

The steep cirque-type fingers of the glacier transition into the main body of the glacier at elevations of about 3,720 to 3,780 m (Meier, 1951). The main body of the glacier has an entirely different set of characteristics from the upper portions. The main body of the glacier is relatively flat, with few deep crevasses. Superglacial streams are in abundance on the main body of the glacier in the late summer months. These streams can often reach depths of several feet and are often as wide as five feet.

3.0 Data and Methods

The current research utilizes a hierarchical method with three levels of monitoring intensity (Figure 3). The primary network (42 glacial complexes) was examined using remote sensing techniques (Landsat imagery) to identify spatial and temporal (1985 to 2005) trends in area change associated with the glaciated region. The results from the Landsat imagery area analysis were then utilized in area-volume scaling techniques (Bahr et al., 1997) to determine glacial volume change.

Next, the secondary network of glaciers (e.g., Mammoth, Minor, Sourdough, Dinwoody, Bull Lake Complex, Knife Point) was chosen and area trends were documented using a combination of aerial photographs and Landsat images for comparison and verification purposes. The Bull Lake Complex of glaciers includes, Bull Lake, Upper Fremont, Sacagawea and Helen Glaciers. It was decided to study these four glaciers as a single complex due their close proximity and common boundaries. The boundaries of each of these glaciers were difficult to discern from satellite images or aerial photographs because they are often connected, and only identifiable by the direction of ice movement. This resulted in the secondary network of glaciers being studied more rigorously than the 42 glacial complexes. Additionally, the use of the aerial photographs extended the period of record back by 20 years (1966 to 2001).

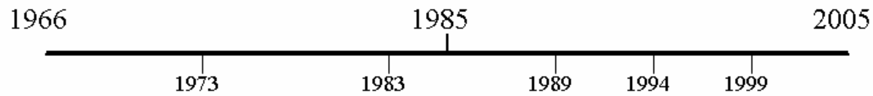

Period of Record:	**1966 to 2001 (36 years)**		**1985 to 2005 (21 years)**	
Data Source:	**USGS Aerial Photos**		**Landsat Imagery**	
Glacial Complexes:	**Green River Drainage**	**Wind River Drainage**	**Green River Drainage**	**Wind River Drainage**
	Mammoth	Dinwoody	12 Glacial Complexes	30 Glacial Complexes
	Minor	Bull Lake Complex		
	Sourdough	Knife Point		
Results:	Area change for 6 Glacial Complexes from 1966 to 2001		Area and Volume change for 42 Glacial Complexes from 1985 to 2005	

Figure 3: Description (dates, sources, glacial complexes, results) of datasets used for the primary and secondary networks of glaciers analyzed.

Finally, a benchmark glacier (Dinwoody Glacier) was chosen and studied intensely through remote sensing data and field measurements. Dinwoody Glacier was chosen as the benchmark glacier, due to the long record of previous studies and its accessibility for ground measurement purposes. Changes in the area and volume of Dinwoody Glacier were estimated, via remote sensing techniques and field measurements. The hierarchical technique used for studying the Wind River Range glaciers is similar to the strategies utilized by Fountain (1997) for analyzing a large network of glaciers

The primary network (42 glacial complexes) of glaciers and the benchmark glacier were analyzed for volume changes over time utilizing the Bahr et al. (1997) area-volume scaling methods. The results of the Dinwoody Glacier stereopair analysis were compared to volume estimates made using the Bahr et al. (1997) techniques in order to verify the Bahr et al (1997) methods.

3.1 Area analysis using Landsat satellite imagery (1985 to 2005) for 42 glacial complexes

For this study, five Landsat satellite images were obtained from the Wyoming Geographic Information Science Center (WyGISC) in Laramie, Wyoming. Each of the images contains the entire Wind River Range and its surrounding areas (Path 37, Row 30). Each of the images was collected during the late summer months while perennial snow cover is at a minimum. Landsat Data was collected for 1985, 1989, 1994, 1999 and 2005, (Table 2) although the 1999 data was not used for this analysis due to early snow cover.

Table 2: Satellite Imagery (Image ID, Date and Platform) utilized for analysis of glacial area changes for 42 glacial complexes from 1985 to 2005.

Image ID	Date	Platform
5037030008522010	Aug. 8, 1985	Landsat 5
5037030008924710	Sept. 4, 1989	Landsat 5
5037030009422910	Aug. 17, 1994	Landsat 5
7037030009925150	Sept. 8, 1999	Landsat 7
5037030000524310	Aug. 31, 2005	Landsat 5

Landsat 5 and Landsat 7 are both equipped with an improved imaging system called a Thematic Mapper (TM). The TM has seven spectral bands ranging from 0.45 to 12.5 µm. Bands 1 through 5 and 7 are in the visible, near infrared and middle infrared wavelength regions and have a ground resolution of 30m. Band 6 is in the thermal infrared wavelength region has a resolution of 120m. Band 5 is especially useful for distinguishing between clouds and snow.

Although the resolution of 30m (Landsat TM) is not ideal for quantitative area measurements, it was found by Meier (1973) that the resolution is adequate to determine the accumulation area ratio on small glaciers, thus it is deemed suitable for estimating the total area of small glaciers (Meier, 1973; Hall and Martinec, 1985). The accumulation area ratio is defined as the ratio between the accumulation area and the ablation area, which can provide some insight to the current state of a glacier.

Despite the relatively course resolution of Landsat images, the advantages of using the Landsat 5 and 7 platforms far outweigh the disadvantages. There was no need to perform tedious procedures to georeference the images since they were already geo-referenced (i.e. have spatial coordinates assigned to them). Also, the 180 km swath width is ideal for analyzing large glaciated regions, without having to rectify and mosaic many aerial photos.

Each Landsat image was analyzed using an unsupervised classification. An unsupervised classification is non-biased statistical approach used to group the pixels of an image into classes for land cover analyses. This procedure can be performed digitally using several different software packages. For this study, ERDAS Imagine was used to perform unsupervised classifications on each of the Landsat images. Due to the large area of coverage for each Landsat image, many classes were necessary to accurately classify each land-cover type. The Landsat image contains areas of agricultural land, forested areas, granite rocks, snow, glacial ice etc, thus 25 classes were chosen to perform the unsupervised classification. In each of the land-cover types mentioned above, several sub-classes may be contained, for example, glacial ice can occur in the form of clean snow from the previous year, firn (a substance that is undergoing the transition from snow to glacier ice), clean glacier ice and dirty glacier ice. Therefore it was necessary to have many classes to be able to identify the subtle differences between different materials.

Each classified Landsat image was then imported to a Geographical Information System (GIS) for further analysis. Each polygon that was classified as glacier ice, using ERDAS Imagine, was digitized in ArcGIS. After each polygon (representing a glacier) was digitized, ArcGIS was used to calculate the surface area of each polygon. Since clouds are similar in color to snow and ice each cloud was identified using the band 5 information and removed by clipping them in ArcGIS.

3.2 Volume analysis for 42 glacial complexes

Utilizing methods presented by Bahr et al. (1997), glacial ice volumes can be estimated from other known quantities such as surface area, thus eliminating expensive, time consuming methods such as detailed radio echo soundings. This approach allows the estimation of ice volumes for glaciers given some simple surface characteristics of each glacier. The Bahr et al. (1997) methods are based upon a study of 144 mountain glaciers, each having reliable radio echo soundings of ice volume. Glaciers from Europe, North America, Central Asia and the Arctic were studied and a scaling analysis of the mass and momentum conservation equations showed that glacier volumes can be related by a power law to glacier surface area which is more easily observed (Bahr et al. 1997). This study found that glacier volumes (in m^3) can be expressed as

$$V = \alpha A^{\beta}$$

where α and β are empirically derived constants and are equal to 0.175 and 1.36, respectively and A is equal to the surface area of the glacier in m^2.

3.3 Area analysis using Aerial Photography (1966-2001) for six glacial complexes

The secondary network of glaciers was analyzed using aerial photos obtained from the Earth Resources Observation and Science (EROS) data center in Sioux Falls, South Dakota, and the Geology Library on the campus of the University of Wyoming, Laramie, Wyoming. The data sets collected include aerial photographs from 1966, 1973, 1983, 1989 and 2001 (Table 3). Aerial Photographs were taken during the summer of 2006, but the data was not available at the time of this study.

Table 3: Aerial Photography (Glacial Complex name, Date, Data Source, Project, Roll and Frame) utilized for analysis of glacial area changes for six glacial complexes (secondary network) from 1966 to 2001.

	Bull Lake Complex				**Dinwoody Glacier**			
	Source	**Project**	**Roll**	**Frame**	**Source**	**Project**	**Roll**	**Frame**
1966	USGS	VBMB	3	44	USGS	VBMB	3	65
1973	NASA	248	26	206	NASA	248	26	207
1983	USGS	NHAP82	397	41	USGS	NHAP82	379	130
1989	USGS	NAPP	1722	5	USGS	NAPP	1722	28
2001	USGS	NAPP	12540	73	USGS	NAPP	12540	94
	Mammoth Glacier				**Sourdough Glacier**			
	Source	**Project**	**Roll**	**Frame**	**Source**	**Project**	**Roll**	**Frame**
1966	USGS	VBMB	3	65	USGS	VBMB	3	81
1973	NASA	248	26	206	NASA	248	26	205
1983	USGS	NHAP82	379	129	USGS	NHAP82	379	131
1989	USGS	NAPP	1722	28	USGS	NAPP	1722	26
2001	USGS	NAPP	12540	94	USGS	NAPP	12540	95
	Knife Point Glacier				**Minor Glacier**			
	Source	**Project**	**Roll**	**Frame**	**Source**	**Project**	**Roll**	**Frame**
1966	USGS	VBMB	3	43	USGS	VBMB	3	65
1973	NASA	248	26	207	NASA	248	26	206
1983	USGS	NHAP82	397	42	USGS	NHAP82	379	129
1989	USGS	NAPP	1722	4	USGS	NAPP	1722	27
2001	USGS	NAPP	12540	73	USGS	NAPP	12540	94

The geo-referencing process involved in performing quantitative analyses of aerial photographs can be prohibitively expensive and time consuming, (Granshaw and Fountain, 2006) thus it was decided to use aerial photographs for analyses on only the benchmark glacier (Dinwoody) and the secondary network.

While the extensive time involved in analyzing aerial photographs makes them disadvantageous, the higher resolution makes them suitable for analyzing a select number of glaciers. The ground resolution of aerial photographs is typically between one and five meters. Unlike Landsat data, which has 180 km swath width, aerial photographs cover small areas of land with each frame (the area covered is dependent upon the focal length and flying height of the camera), thus many aerial photographs are required to study large areas.

The methods used to estimate glacier surface area using aerial photographs were similar to those used for Landsat data, once the digitizing and geo-referencing processes were complete. Each of the aerial photographs obtained from the Geology Library were in the form of paper photographs and films, while each image from the EROS Data Center was pre-digitized. Each paper photograph was scanned using a high resolution photo scanner and each of the films obtained was scanned using a high resolution film scanner. The high resolution film scanner is similar to a photo scanner, except that light is provided on only one side of the film while the other side is kept dark, thus illuminating the features contained in the film.

The geo-referencing process involves assigning spatial coordinates to the photo. This process was completed using ArcGIS. Typically, spatial coordinates were provided for several points on each photo (usually the four corner points and the center coordinates). After assigning spatial coordinates to several points on the photograph, spatial coordinates can be estimated for any point on the photo by determining the spatial coordinate's location relative to known points. Geo-referencing was performed with a threshold root mean square error (RMSE) of 0.0003 meters. Once digitizing and geo-referencing was complete, the photos were imported into ERDAS Imagine and classified, using a process similar to that used for the Landsat data. Since the aerial photos cover a relatively small area of land when compared to the Landsat data, there was less variability of materials on the surface, thus fewer classes were needed. For analysis of the secondary glacier network, 15 classes were used and the area of the resulting polygons, representing glacier areas, was calculated using ArcGIS.

3.4 Stereo analysis of USGS aerial photos for Dinwoody Glacier

In addition to calculating surface area for the secondary network, aerial photographs were used to calculate the change in volume of Dinwoody Glacier from 1983 to 2001 (Table 4). Stereo photogrammetry is a method used to gain elevation data from a pair of aerial photographs of the same object, taken from different positions. Traditional methods of stereo photogrammetry require the pair of aerial photos to be viewed under a stereo zoom transfer scope, with a vertical measurement module.

Table 4: Aerial Photography (Date, Data Source, Project, Roll and Frame) utilized for analysis of glacial volume changes for Dinwoody Glacier

Year	Source	Project	Roll	Frame
1983	USGS	NHAP82	379	129
	USGS	NHAP82	379	130
2001	USGS	NAPP	12540	93
	USGS	NAPP	12540	94

This method is very tedious and time consuming. Modern techniques allow this process to be completed digitally with the use of a photogrammetry software package. For the current study, Leica Photogrammetry suite was used to create the block files, view the overlapping portion of the images in 3-D, and make vertical measurements.

A stereo block file is a set of two or more photos with overlapping portions, which are positioned such that the parallax between the common objects allows the user to view the objects in 3-D using either red/blue anaglyph stereo glasses or LCD stereo glasses that work in conjunction with an emitter. The creation of a stereo block file includes specifying interior and exterior orientation information about the photos being used. The interior orientation is defined as the orientation of the film (or other recording media) in relation to the sensor. The exterior orientation is defined as the orientation of objects on the ground in relation to the sensor. Once interior and exterior orientations are defined, the user can generate tie points (points that are of the same spatial coordinates on each photo). For this study 100 tie points were typically generated. Once the user has generated tie points on each photo, triangulation is performed, which is the process by which the stereo model calculates the elevation of each point on the photo via triangulation with other points of known elevation (control points). Since glaciers move, each control point was strategically located on a distinct rock feature or another object, not within the glacier boundaries, that is not prone to moving (changing elevation) over time. Triangulation was repeated until the RMSE was below 3m on each stereo block file. The parallax between common objects on different photos is very sensitive in areas of high relief, thus it is imperative to adjust the parallax between two photos often when making vertical measurements across broad areas.

3.5 Field Data collected from Dinwoody Glacier

Field measurements of Dinwoody Glacier were collected as verification data for the satellite and aerial photograph analyses of this project. The fieldwork performed involved (1) mapping of the surface area, elevations and ice margins of Dinwoody Glacier using GPS, (2) estimating the volume of ice remaining via ice depth measurements across Dinwoody glacier and (3) obtaining ground photographs of the glacier and surrounding areas for comparison to other photographs taken of the area, which provided valuable qualitative data.

The field reconnaissance work was performed August 6-12, 2006. Dinwoody Glacier was accessed via the United States Forest Service (USFS) Glacier trail, starting at Trail Lake Ranch near Dubois, Wyoming. Due to the distance required to travel and the large amount of gear and research equipment needed, a local outfitter was hired to provide transportation of gear and equipment to the field site. The first day of travel included an approximately 26 km hike to the outfitters base camp at Downs Fork. The second day of travel required an approximately 16 km hike to the upper portion of Floyd Wilson Meadows, where the research team set up a base camp for the remaining days. The research base camp was located approximately 6 km from the terminus of Dinwoody Glacier. Due to accessibility issues this 6 km stretch was traveled only by foot and all gear was transported by members of the research team. The following three days were occupied with taking GPS elevation measurements, ice-depth measurements and ground photographs, followed by two consecutive days of travel from the research base camp to the trailhead at Trail Lake Ranch. Tables showing field personnel and field equipment used are available in Appendices 1 and 2.

The GPS survey of Dinwoody Glacier was completed by collecting 110 real-time differential GPS points on the glacier (Figure 4). The locations of the GPS readings are provided in Appendix 3.

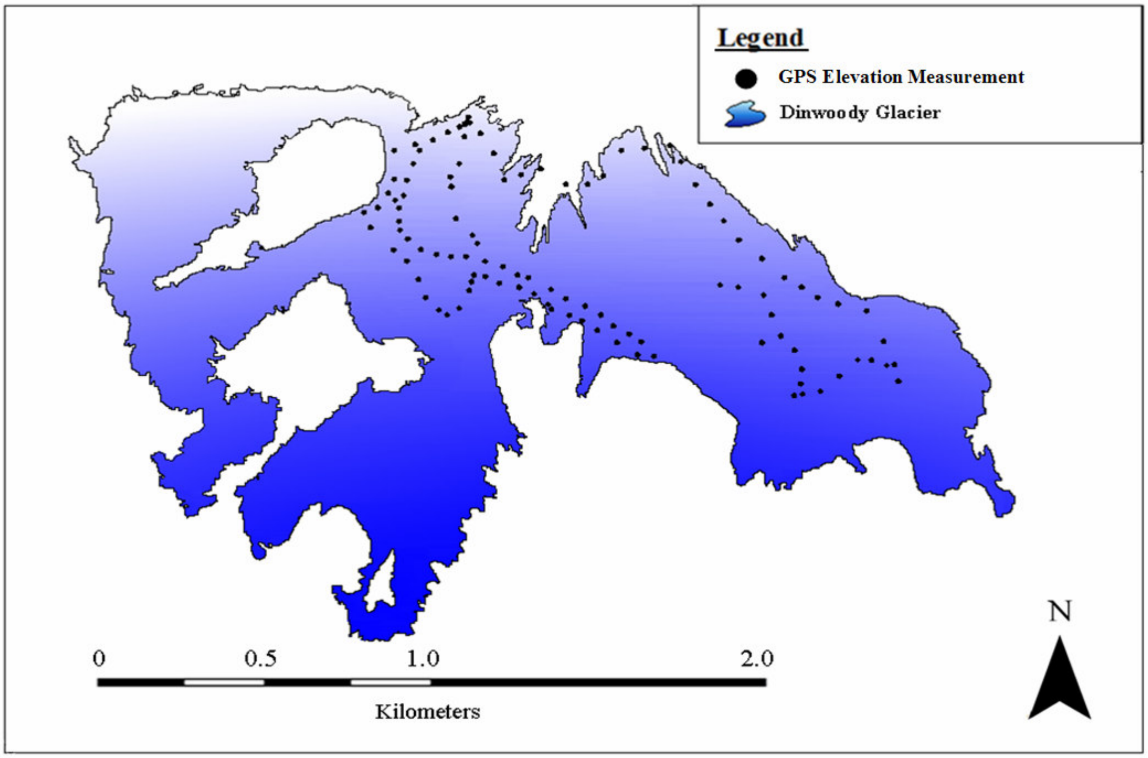

Figure 4: Locations of GPS elevation readings. All GPS readings were collected during the 2006 field efforts for this study

Survey data was collected using two Trimble ProXRS GPS units. One of the units was utilized as a base unit, which was kept at a stationary location, while the other unit was utilized as a rover. By keeping one unit (the base unit) stationary, accurate GPS locations and elevations were obtained since the rover unit was able to utilize the position of the base in the trilateration process, thus lessening the distance between the rover and a GPS with known coordinates and elevation. The GPS survey was generally conducted after 11:00 a.m. mountain standard time due to the availability of satellite signals.

The depth of ice was measured at 150 different points along a single traverse across the main body of the glacier (Figure 5). Locations of each ice-depth measurement are provided in Appendix 4.

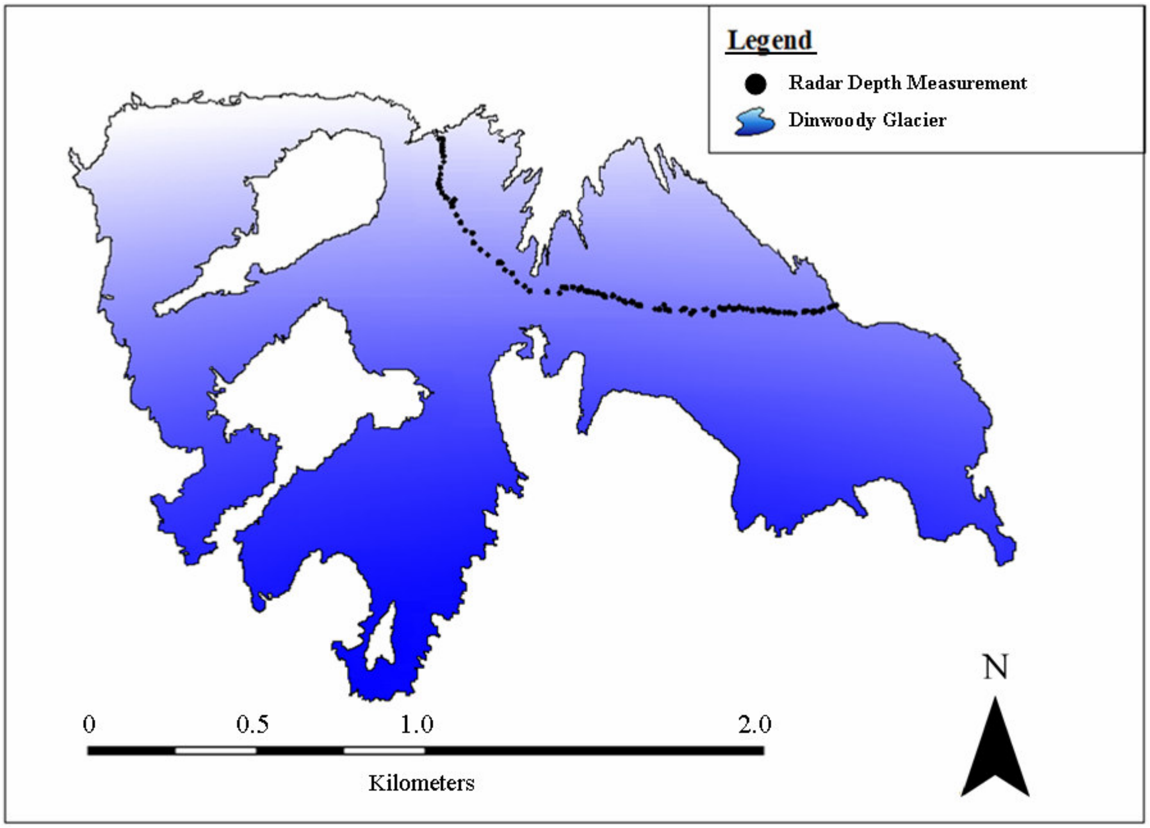

Figure 5: Locations of radar ice depth measurements. All ice depth measurements were collected during the 2006 field efforts for this study

The ice depth was measured using a radar unit that consisted of a 5mHz antenna with a 5m offset between the source and the receiver. The receiver consisted of an oscilloscope that was triggered by the arrival of the 5mHz wave that traveled through the air. Once the wave was initially received by the oscilloscope it was directed downward through the ice until it was reflected from the bedrock and moved upwards back through the ice. The amount of time elapsed between the reception of the two waves was measured, which was then correlated to an ice depth measurement using a typical value for wave speed through ice. The approximate locations of each ice depth measurement were recorded using a handheld GPS unit. A handheld unit was used because of the longer battery life as compared to the Trimble ProXRS unit.

The remotely sensed data and field data was analyzed to quantify the glacial meltwater contributions to downstream flows. Three unimpaired USGS streamflow stations were identified and the contributing watershed boundaries were delineating using ArcHydro. The glacial volume change for each of the contributing glaciers was averaged over the 25 year period and compared to warm season flow volumes from each of the streamflow gaging stations. The warm season was identified as the four month period from July 1 to October 31, and was analyzed exclusively since nearly all glacial ablation occurs during this period. By comparing the average glacial loss from 1985 to 2005 to streamflow statistics, an estimated contribution of glacial meltwater was determined.

4.0 Results

4.1 Glacial area change for 42 glacial complexes from 1985 to 2005

The average change in surface area (% of baseline 1985 surface area) for the 42 glacial complexes of the Wind River Range from 1985 to 2005 was a decrease of 37%. It has been noted in previous studies that glaciers of smaller area are typically more sensitive to changes in climate than large glaciers (Granshaw & Fountain, 2006). Of the 42 glacial complexes analyzed, 25 had an area of less than 0.5 km^2 in 1985, while 17 were greater than 0.5 km^2 in 1985. The glacial complexes with a surface area less than 0.5 km^2 experienced an average surface area loss (% of baseline 1985 surface area) of 43%, while the large glaciers (greater than 0.5 km^2) experienced an average surface area loss of 28% (Table 5 and Figure 6).

Table 5: Surface area (km^2) measurements for 42 glacial complexes (1985, 1989, 1994 and 2005).

		Glacier Surface Area (km^2)			
Site ID	**Glacier Names**	**1985**	**1989**	**1994**	**2005**
1	NN	0.20	0.19	0.13	0.14
2	NN	0.38	0.33	0.24	0.21
3	NN	0.21	0.19	0.17	0.15
4	NN	0.28	0.28	0.22	0.18
5	Harrower Glacier	0.27	0.20	0.19	0.17
6	NN	0.36	0.30	0.20	0.18
7	Knife Point Glacier	1.49	1.27	1.09	1.11
8	NN	0.28	0.22	0.17	0.10
9	Bull Lake Glacier	8.00	7.74	7.16	6.87
	Upper Fremont Glacier				
	Sacagawea Glacier				
	Helen Glacier				
10	NN	0.35	0.30	0.24	0.16
11	Stroud Glacier	0.59	0.48	0.39	0.37
12	Twins Glacier	0.79	0.60	0.55	0.49
	NN				
13	NN	0.16	0.16	0.16	0.10
14	Mammoth Glacier	2.78	2.22	2.25	2.04
15	Baby Glacier	0.29	0.19	0.20	0.19
16	NN	0.18	0.15	0.10	0.09
17	Dinwoody Glacier	2.98	2.71	2.61	2.59
	NN				
18	Heap Steep Glacier	0.16	0.10	0.10	0.06
19	NN	0.37	0.37	0.24	0.19
20	NN	0.23	0.23	0.14	0.12
21	NN	0.22	0.21	0.18	0.16
22	Minor Glacier	0.69	0.47	0.46	0.42
23	Gannett Glacier	4.14	3.92	3.58	3.28
	Gooseneck Glacier				
	NN				
24	Grasshopper Glacier	3.59	3.49	3.35	2.82
25	J Glacier	0.34	0.28	0.25	0.23
26	Sourdough Glacier	1.52	1.20	1.15	1.00
27	NN	0.22	0.23	0.17	0.13
28	NN	0.39	0.39	0.33	0.28
29	NN	0.81	0.74	0.73	0.58
	NN				
30	Connie Glacier	0.68	0.49	0.49	0.43
31	NN	0.76	0.64	0.65	0.52
32	Downs Glacier	1.09	0.95	0.97	0.81
	NN				
	NN				
33	NN	0.27	0.23	0.21	0.15
34	NN	0.95	0.90	0.93	0.68
	NN				
35	Continental Glacier	3.57	3.41	3.53	2.84
	NN				
	NN				
36	NN	0.38	0.35	0.33	0.29
37	NN	0.55	0.53	0.49	0.38
38	NN	0.19	0.17	0.15	0.11
39	NN	0.12	0.09	0.07	0.05
40	NN	0.16	0.15	0.11	0.11
41	NN	0.10	0.08	0.05	0.03
42	NN	0.06	0.05	0.04	0.02

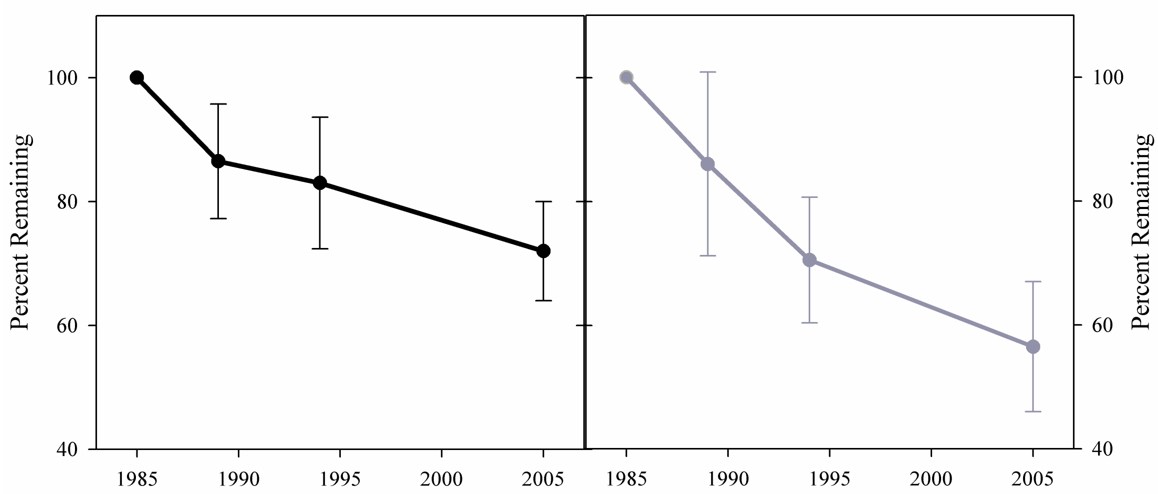

Figure 6: Surface area variations from 1985 to 2005 (percent of 1985 surface area) for 42 glacial complexes in the Wind River Range. The average loss for large (greater than 0.5 km2) glacial complexes are identified on the left by a black line (with standard deviations shown) while small (less than 0.5 km2) glacial complexes are identified on the right by a grey line.

It was found that the glaciers located in the central portion of the glaciated area of the Wind River Range experienced a smaller decrease in surface area than the glaciers on the northern or southern portion of the region (Figure 7). This difference in magnitude of loss could be attributed to the number of large glaciers located in the middle portion of the glaciated region. The spatial variability of glacier size appears to be the cause for spatial variability in glacier loss.

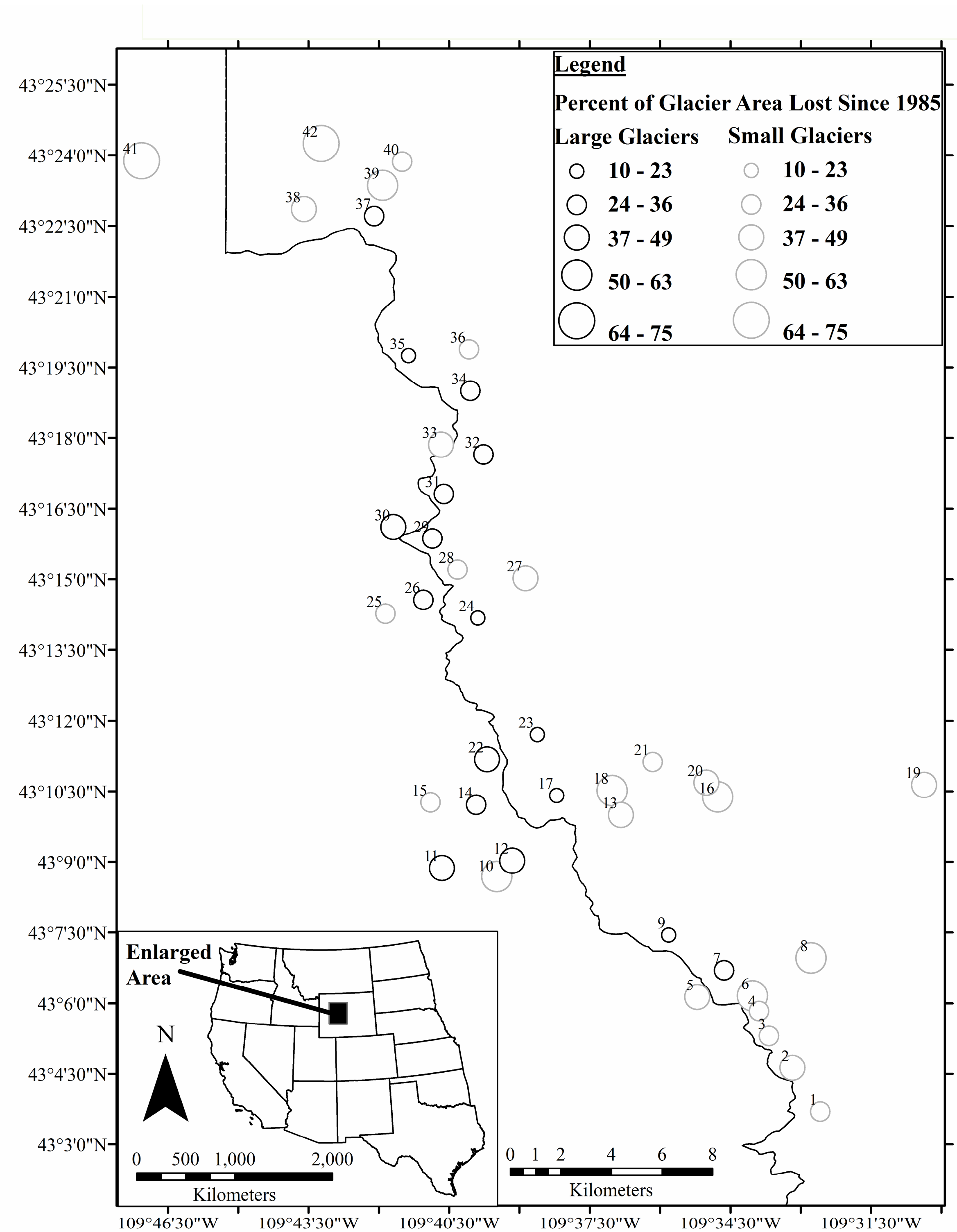

Figure 7: Total surface area change from 1985 to 2005 (percentage of baseline 1985 area) for 42 glacial complexes in the Wind River Range. Large (greater than 0.5 km2) glacial complexes are identified by a black circle while small (less than 0.5 km2) glacial complexes are identified by a grey circle.

4.2 Glacial volume change for 42 glacial complexes from 1985 to 2005

Applying area-volume scaling techniques per Bahr et al. (1997), yearly (1985, 1989, 1994 and 2005) ice volume in million cubic meters ($m^3 \times 10^6$) was calculated for all 42 glacial complexes (Table 6). While significant area loss was noted for small (surface area less than 0.5 km^2) glaciers, significant volume loss was identified for large (surface area greater than 0.5 km^2) glaciers (Figure 8). The total estimated volume of ice lost from 1985 to 2005 for the 42 glacial complexes was 410 $m^3 \times 10^6$.

Table 6: Volume (m^3 x 10^6) measurements for 42 glacial complexes for 1985, 1989, 1994 and 2005 based on Bahr et al. (1997).

		Glacier Volume (m^3 x 10^6)			
Site ID	**Glacier Names**	**1985**	**1989**	**1994**	**2005**
1	NN	2.8	2.7	1.5	1.7
2	NN	6.7	5.5	3.7	3.1
3	NN	3.0	2.7	2.3	1.9
4	NN	4.4	4.5	3.3	2.5
5	Harrower Glacier	4.2	2.9	2.6	2.3
6	NN	6.4	4.9	2.7	2.4
7	Knife Point Glacier	43.5	35.0	28.3	29.1
8	NN	4.6	3.2	2.3	1.2
9	Bull Lake Glacier	428.0	409.3	367.6	347.6
	Upper Fremont Glacier				
	Sacagawea Glacier				
	Helen Glacier				
10	NN	6.2	4.9	3.6	2.1
11	Stroud Glacier	12.3	9.2	7.0	6.6
12	Twins Glacier	18.3	12.5	11.3	9.6
	NN				
13	NN	2.0	2.1	2.0	1.1
14	Mammoth Glacier	101.5	74.9	76.2	66.6
15	Baby Glacier	4.8	2.6	2.9	2.6
16	NN	2.4	2.0	1.1	1.0
17	Dinwoody Glacier	111.8	98.2	93.2	92.5
	NN				
18	Heap Steep Glacier	2.1	1.1	1.1	0.6
19	NN	6.6	6.5	3.6	2.7
20	NN	3.3	3.5	1.8	1.4
21	NN	3.3	2.9	2.5	2.1
22	Minor Glacier	15.2	9.1	8.7	7.7
23	Gannett Glacier	174.6	161.9	143.5	127.1
	Gooseneck Glacier				
	NN				
24	Grasshopper Glacier	144.0	138.6	131.2	103.4
25	J Glacier	5.8	4.5	3.8	3.4
26	Sourdough Glacier	44.9	32.5	30.7	25.2
27	NN	3.2	3.4	2.4	1.5
28	NN	7.0	6.9	5.7	4.5
29	NN	18.9	16.8	16.5	12.0
	NN				
30	Connie Glacier	15.1	9.6	9.5	8.0
31	NN	17.5	13.7	13.9	10.3
32	Downs Glacier	28.5	23.4	24.4	18.8
	NN				
	NN				
33	NN	4.3	3.4	3.1	1.9
34	NN	23.7	21.8	22.9	15.1
	NN				
35	Continental Glacier	143.0	134.1	140.7	104.8
	NN				
	NN				
36	NN	6.7	6.2	5.6	4.6
37	NN	11.1	10.7	9.7	6.9
38	NN	2.6	2.3	1.8	1.3
39	NN	1.5	0.9	0.7	0.5
40	NN	2.2	1.9	1.3	1.2
41	NN	1.1	0.8	0.4	0.2
42	NN	0.5	0.4	0.3	0.1

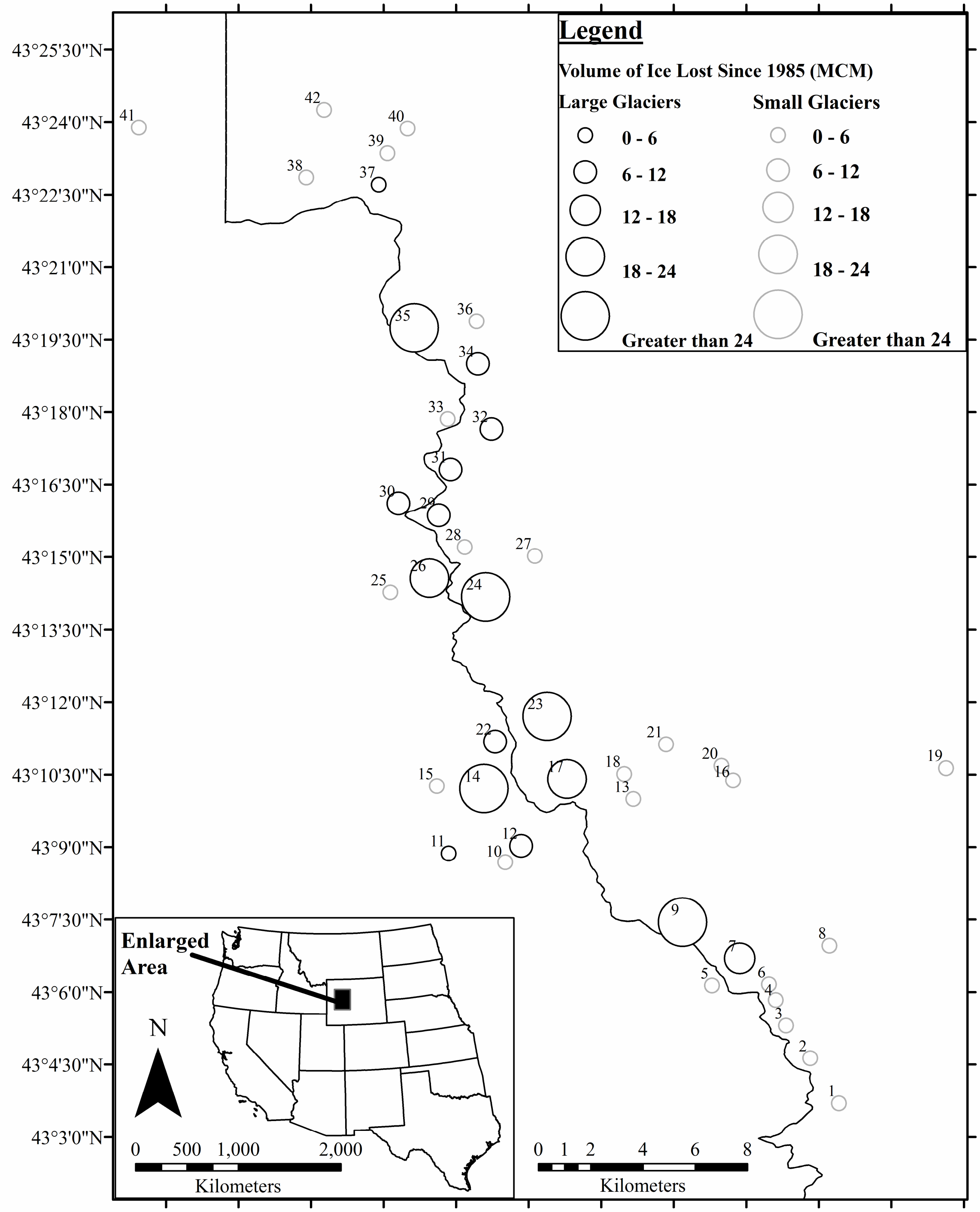

Figure 8: Total volume loss (million cubic meters) from 1985 to 2005 for 42 glacial complexes in the Wind River Range based on Bahr et al. (1997). Large (greater than 0.5 km^2) glacial complexes are identified by a black circle while small (less than 0.5 km^2) glacial complexes are identified by a grey circle.

The volume change results (from the Bahr et al. (1997) methods) indicate that a significant amount of ice has been lost from the Wind River Range glaciers. Assuming that the density of ice is 90% that of water, 410 $m^3 \times 10^6$ of ice loss translates into a loss of approximately 370 $m^3 \times 10^6$ of water equivalent. The majority of the water lost from Wind River Range glaciers contributes to three watersheds defined by USGS streamflow gages, Dinwoody Creek Above Lakes, Bull Lake Creek Above Bull Lake and Green River at Warren Bridge (Figure 9).

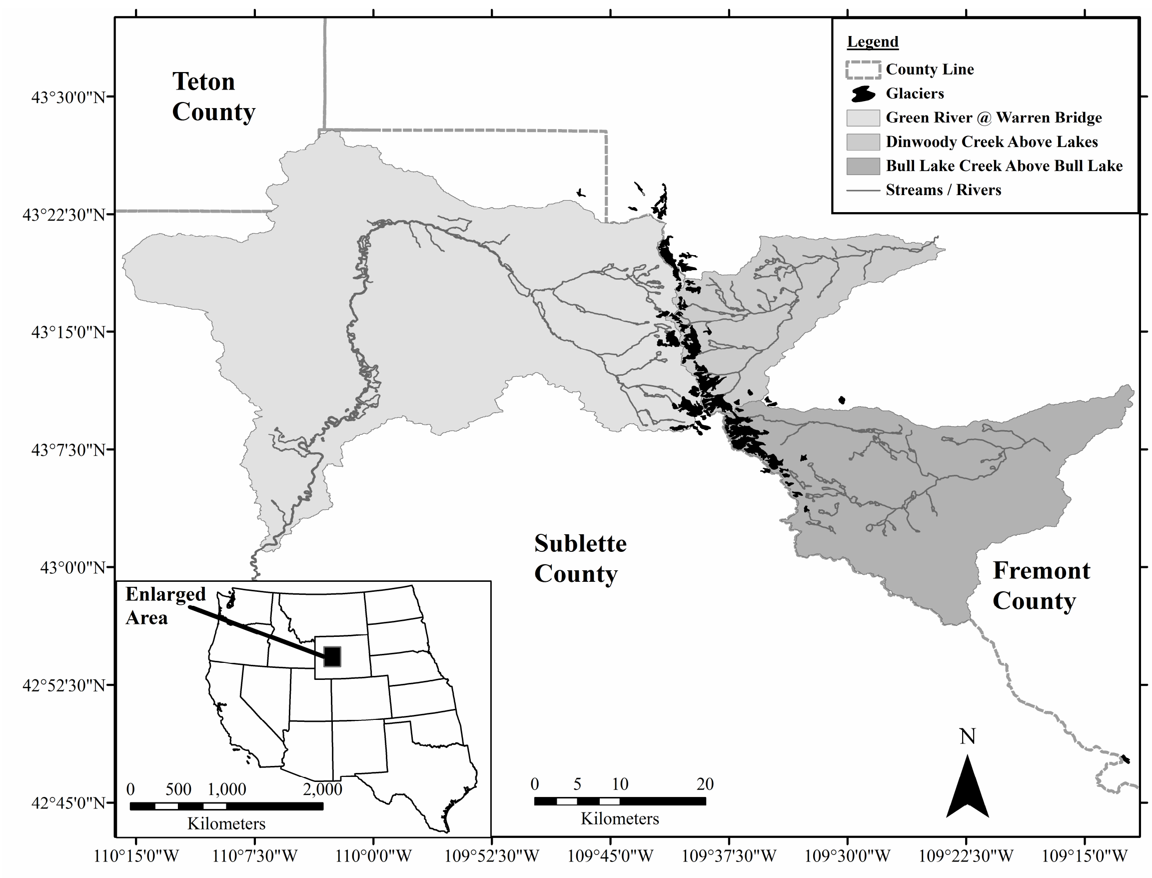

Figure 9: The three primary watersheds that have glacial meltwater contributions to streamflow and the glaciers that contribute to them. Glaciers are showm in black, while watershed boundaries are shown in different shades of grey.

The watershed area contributing to streamflow at the Green River at Warren Bridge streamflow gage contains seven glacial complexes. Assuming uniform melt rates from 1985 to 2005, it was determined that the average warm season glacial contributions to streamflow for this gage are 24 cubic meters per minute (m^3/min). For this study, the warm season is defined as the four month period from July through October, and it was assumed that all glacial melt takes place during this period. The average annual warm season flows from 1985 to 2005 at the Green River at Warren Bridge gage is 506 m^3/min.

The Dinwoody Creek Above Lakes gage has a watershed containing ten glacial complexes, which contribute approximately 40 m^3/min of flow to the recorded streamflow at that gage. The average annual warm season flow at that gage is 408 m^3/min.

Nine glacial complexes contribute to streamflow at the Bull Lake Creek Above Bull Lake gage site. These glacial complexes contribute approximately 32 m^3/min to the total streamflow at the streamflow gage. The annual average warm season flow at that gage is 603 m^3/min (Table 7). Each of the previous glacial contribution estimates assume that all of the volume lost from the glaciers is conveyed to its respective streamflow gage and that no water is lost to infiltration (groundwater) or evaporation.

Table 7: Percent contribution of glaciers to streamflow for three USGS unimpeded streamflow gages.

Gage Indentifier	Number of Contributing Glacial Complexes	% Contribution of Glaciers
Green River at Warren Bridge	7	4.7%
Dinwoody Creek Above Lakes	10	9.8%
Bull Lake Creek above Bull Lake	9	5.3%

4.3 Glacial area change for six glacial complexes from 1966 to 2001

The secondary network of glaciers (six glacial complexes), which was analyzed using repeat aerial photography dating back to 1966, experienced an average decrease in size of 46% from 1966 to 2001 (% of 1966 surface area) (Figure 10 and Table 8). The extended period of record gained by using aerial photographs provided a useful tool for analyzing long term trends of glacial behavior in the Wind River Range. Each of the glaciers analyzed in the secondary network were larger than 0.5 km^2, and were all located near the middle portions of the Wind River Range glaciated region. Thus, no significant spatial variation was noted while analyzing the secondary network.

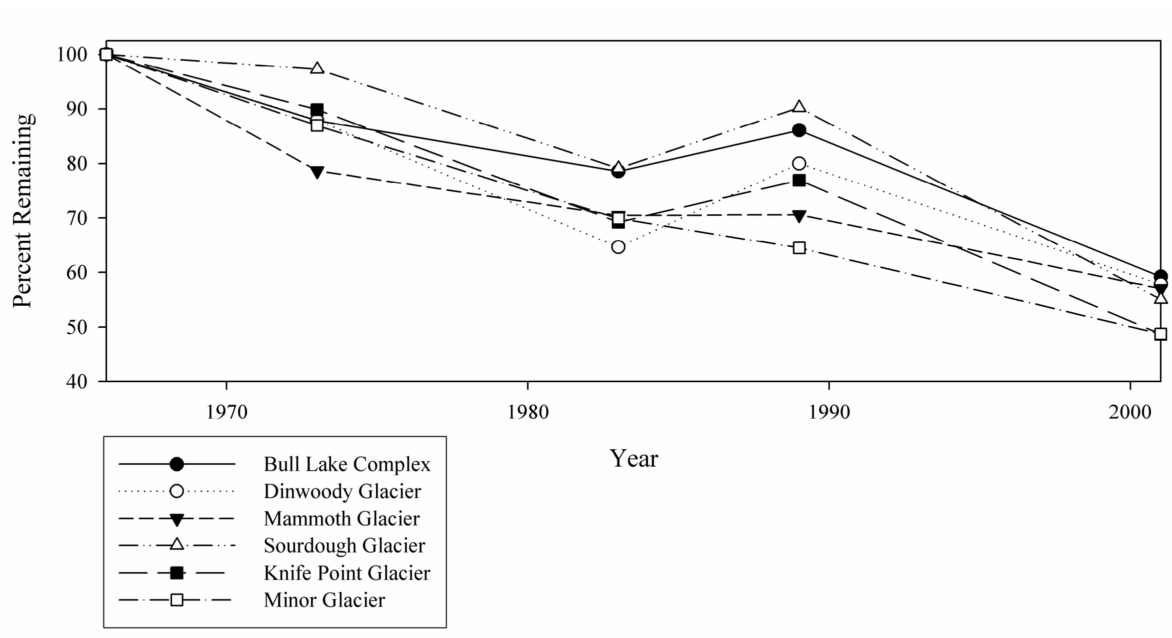

Figure 10: Surface area variations from 1966 to 2001 (percent of 1966 surface area) for 6 glacial complexes in the Wind River Range.

Table 8: Surface area (km2) measurements for 6 glacial complexes (1966, 1973, 1983, 1989 and 2001).

		Glacier Surface Area (km^2)				
Site ID	**Glacier Names**	**1966**	**1973**	**1983**	**1989**	**2001**
7	Knife Point Glacier	1.92	1.72	1.33	1.47	0.93
9	Bull Lake Glacier	10.79	9.48	8.48	9.28	6.38
	Upper Fremont Glacier					
	Sacagawea Glacier					
	Helen Glacier					
14	Mammoth Glacier	4.07	3.20	2.87	2.87	2.32
17	Dinwoody Glacier	4.23	3.72	3.16	3.29	2.38
22	Minor Glacier	0.93	0.81	0.65	0.60	0.45
26	Sourdough Glacier	1.59	1.55	1.26	1.44	0.87

Some differences were noted, between the surface area as calculated via Landsat images and aerial photographs (Table 9). The two datasets (Landsat and aerial photographs) contain a common data point in 1989, thus the two methods can be easily compared. It was found that Landsat consistently underestimated the surface area of each glacier as compared to surface area estimates made using aerial photographs. An average difference in surface area of 18.25% was found between the two methods for the 1989 datasets.

Table 9: Difference in 1989 surface area between Landsat imagery and aerial photographs.

	Surface Area (km^2)		
Glacier	**1989 Aerial Photographs**	**1989 Landsat Imagery**	**Percent Difference**
Bull Lake Complex	9.3	7.7	17
Dinwoody	3.3	2.7	18
Mammoth	2.9	2.2	23
Sourdough	1.4	1.2	17
Knife Point	1.5	1.3	14
Minor	0.6	0.5	21

This difference may be caused by many factors but is most likely due to inherent differences in the two remote sensing platforms used to record the data. Due to the lower resolution (30m) Landsat images can incorporate sizeable amounts of error into an analysis, while most of the error is concentrated near the boundaries of land cover types where the abrupt transition from one type of land cover to another is muted.

4.4 Glacial area change for Dinwoody Glacier

The benchmark glacier (Dinwoody Glacier) was analyzed with the most rigor, using aerial photographs for area and volume changes and field data to verify remotely sensed data. From 1966 to 2001 (using aerial photos), the surface area of Dinwoody Glacier declined by 43% going from 4.24 km^2 in 1966 to 2.38 km^2 in 2001 (Figure 11).

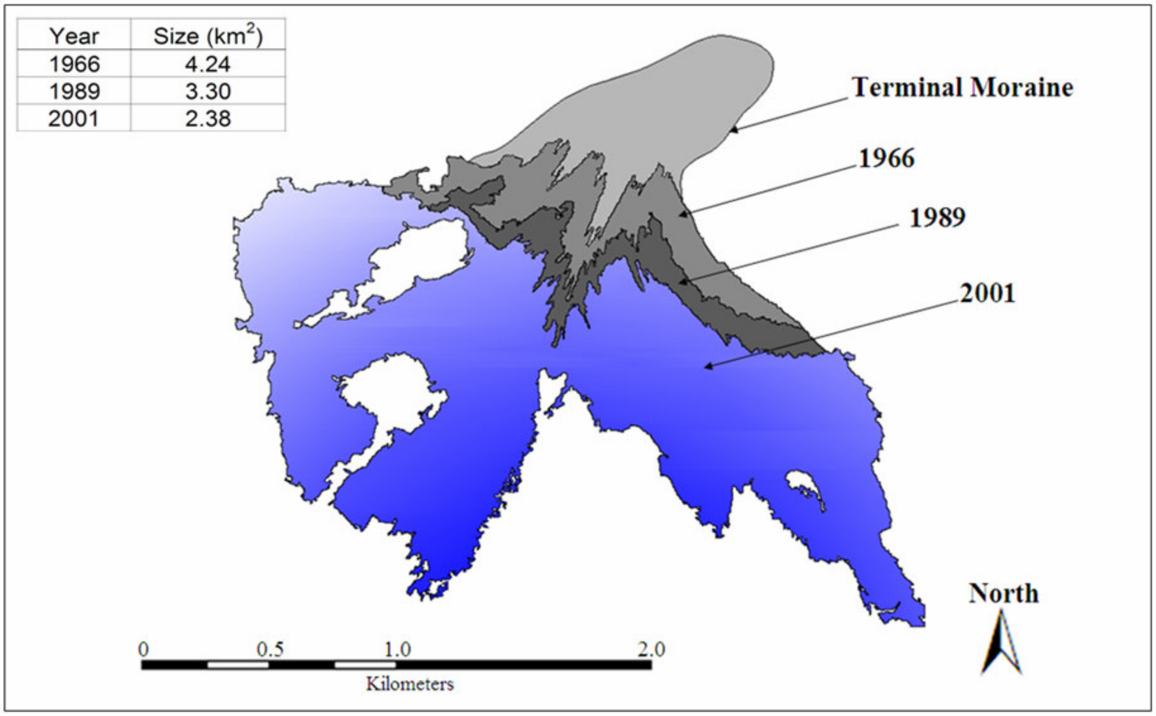

Figure 11: Variation of Dinwoody Glacier Terminus Position and Surface area from 1966 to 2001.

The areas calculated for Dinwoody Glacier in this study were slightly higher than those calculated by Meier (1962) (3.44 km^2), Marston et al. (1991) (2.91 km^2), and Wolken (2000), (2.19 km^2). The discrepancies between the values previously calculated and those calculated in this study could come from a variety of different error sources. Possible error sources include having poor spatial information for photographs used (especially earlier photographs), having photographs that are not taken directly above the glacier (slightly oblique photographs) and user error while geo-referencing the photographs.

Block files were created from aerial photographs for Dinwoody Glacier for 1983 and 2001. A grid system was developed and used to collect elevation data for the glacier. Elevations were read at a 100 meter interval in both the x and y directions. A resolution of 100 meters yielded 500 data points for the glacier and its surrounding areas. The elevation data collected were used to (1) create a topographic map of Dinwoody glacier

(2001), (2) create a three-dimensional representations of the glaciers surface (1983 and 2001) and (3) calculate the volume between the two surfaces (Figures 12, 13 & 14).

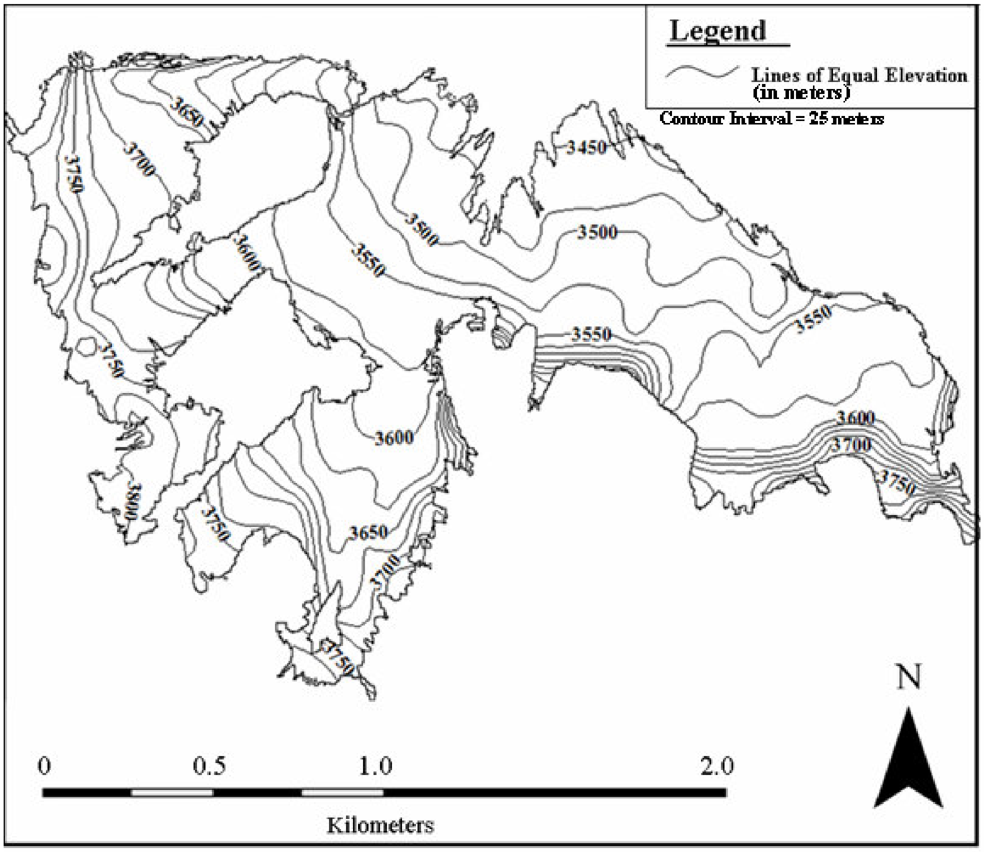

Figure 12: Topographic map of Dinwoody Glacier. The elevation data used was collected from a 2001 stereo block file. (Coordinates are based upon UTM WGS 1984 Zone 12 North projection/datum)

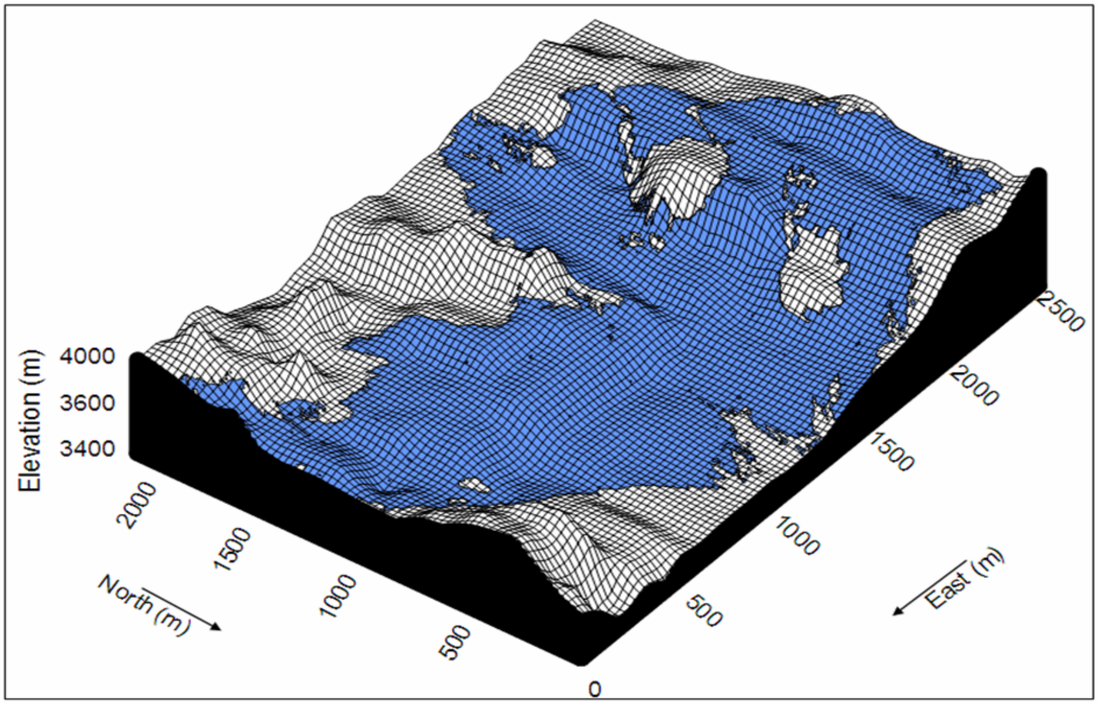

Figure 13: 3-dimensional image of Dinwoody Glacier in 1983.

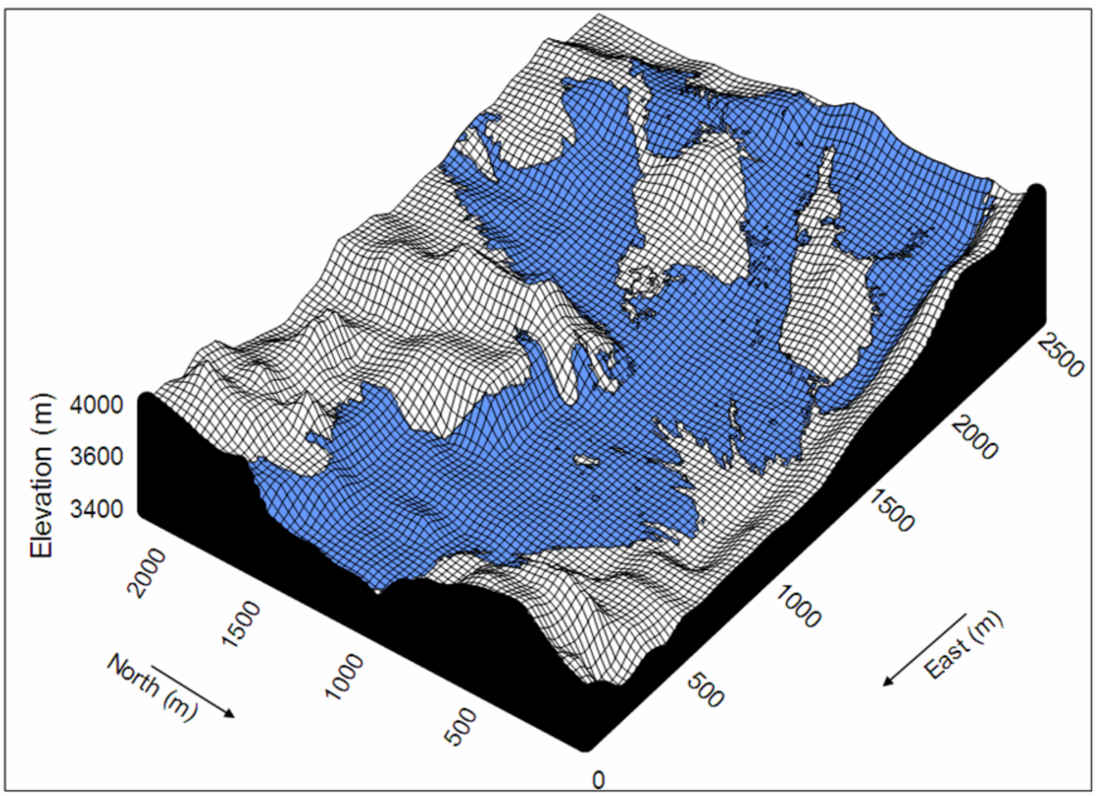

Figure 14: 3-dimensional image of Dinwoody Glacier in 2001.

Dinwoody Glacier lost approximately 66 $m^3 \times 10^6$ of ice during the 18 year period. Assuming an average ice density of 0.90 g/cm^3 (90% that of liquid water) it was determined that Dinwoody Glacier has lost approximately 60 $m^3 \times 10^6$ of water equivalent from 1983 to 2001 (more than 48,500 acre-ft). The amount of ice lost from 1983 to 2001 is nearly equal to the amount of ice lost over the 25 year period between 1958 and 1983 (Marston et al., 1991). Applying area-volume scaling techniques (e.g., Bahr et al., 1997) to the 1983 and 2001 surface areas, the loss of ice volume was calculated to be 39 $m^3 \times 10^6$, which is approximately 40% less than the volume calculated (66 $m^3 \times 10^6$) using aerial photograph stereopairs.

When compared to the differential GPS measurements (taken in 2006) the stereo model, using photographs from 2001, yielded very similar elevation results. The 110 elevations collected using GPS methods and stereo model methods were first tested for normality using the Kolomogorov-Smirnov test (Maidment, 1993). Following the normality test, a paired t-test was performed. The difference in means between the elevations collected via GPS and stereo methods at the same x, y coordinates were not significantly greater than zero at a 90% level ($p < 0.10$) (Navidi, 2006). This result confirms that the stereo models used are acceptable methods for determining glacier elevations and volume changes over time. The results could be improved upon by using more recent aerial photographs (2006), which were not available at the time of this study.

4.5 Analysis of field data

4.5.1 Ice-Depth Data

Marston et al. (1991) estimated that the depth of Dinwoody glacier ranged from 54 to 111 meters. The methods used to estimate ice thickness by Marston et al. (1991)

are similar to those used in the current study, although the locations of readings were not recorded during the 1988 study, thus the traverse used in 1988 could not be exactly duplicated. During the field reconnaissance work in August 2006, a traverse, believed to be as close as possible to that used in 1988, along the central portion of the glacier was made with the 5 mHz antennae to gain updated ice-depth data. Although the locations of readings could not be exactly duplicated, the results have shown that the ice depths from the two dates (1988 and 2006) are very similar (Figure 15).

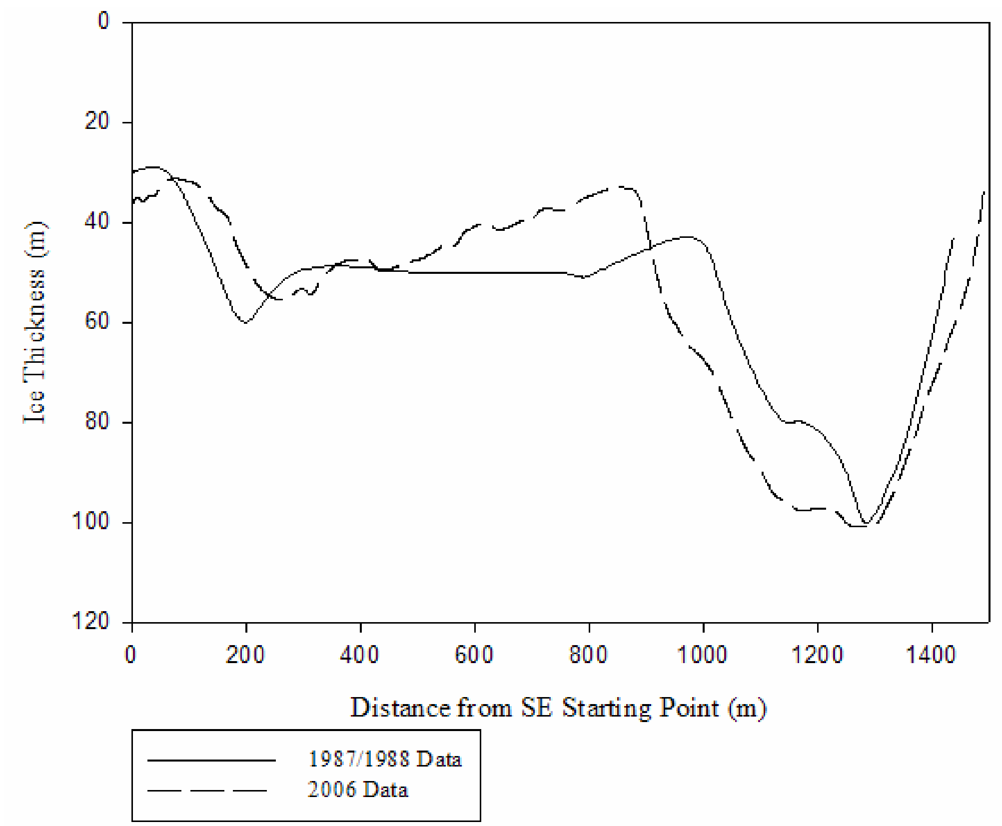

Figure 15: Ice-depth comparisons for Dinwoody Glacier. The 1988 data was obtained from Marston et al. (1991).

It can be seen that according to these data, the glacier has apparently gained ice thickness in some areas and lost thickness in others over the 15 year period between studies, which may be due to error introduced by not being able to duplicate exactly the original traverse, or the redistribution of ice. Since glaciers move under the force of their own weight it is common for the mass of a glacier to be redistributed over time due to the overall movement of ice.

4.5.2 Repeat Terrestrial Photography

Repeat ground (terrestrial) photography provides useful qualitative information regarding the behavior of glaciers and areas of robust change. Photographs of Dinwoody Glacier were taken in 1935, and were made available via the American Heritage Center in Laramie, Wyoming. Photographs taken from the same position as those in 1935 were taken in 1988 by Marston et al. (1991). The 2006 field work also yielded photographs taken from the same position as those from 1935 and 1988 (Figures 16 & 17).

Repeat ground photography is a valuable geomorphic tool for assessing qualitative long term changes in land cover types. Repeat photography can make it possible to assess changes to land cover that either (1) are not apparent to visual inspection or (2) occur over long periods of time, making them hard to ascertain during short-term field efforts (Wilkerson and Schmid, 2003)

Figure 16: Repeat ground photographs showing Dinwoody Glacier in (a) 1935, (b) 1988 and (c) 2006. 1935 photos were obtained from the American Heritage Center in Laramie, Wyoming, 1988 photos were obtained from Marston et al. (1991) and 2006 photos were taken during the 2006 field efforts for this study.

Although it is possible to obtain quantitative information from repeat terrestrial photography, this study utilizes repeat terrestrial photography to gain a qualitative understanding of glacier behavior over time. By inspection, it is apparent that Dinwoody Glacier has undergone significant changes throughout the lower elevations (near the terminus) and has remained relatively stable at higher elevations (near the upper margins). The significant changes near the terminus of the glacier are due to warmer temperatures at lower elevations as well as lower albedo. The snow and ice near the terminus tends to be littered with rocks and dirt, thus lowering the albedo and increasing the effects of solar radiation.

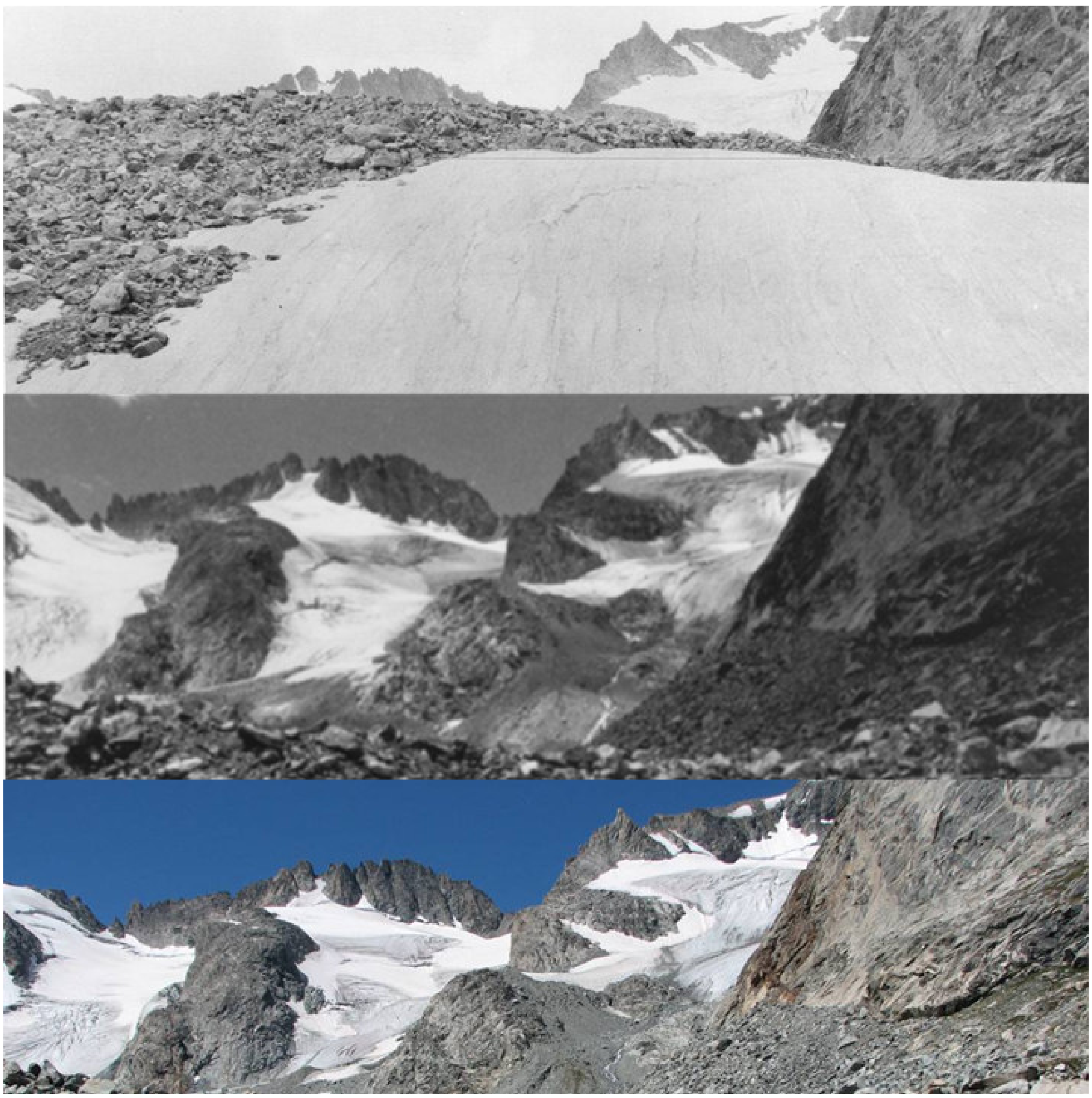

Figure 17: Repeat ground photographs showing Dinwoody Glacier in (a) 1935, (b) 1988 and (c) 2006. 1935 photos were obtained from the American Heritage Center in Laramie, Wyoming, 1988 photos were obtained from Marston et al. (1991) and 2006 photos were taken during the field efforts for this study.

5.0 Conclusions

The results of the research revealed significant area loss for 42 glacial complexes in the Wind River Range from 1985 to 2005 when evaluating Landsat imagery. Smaller glaciers (area less than 0.5 km^2) were impacted greater (e.g., more area loss) when compared to larger glaciers (area greater than 0.5 km^2). This result was consistent with previous research efforts in other glacial regions. When extending the period of record back to 1966 and utilizing other types remote sensing data (i.e., aerial photographs), the results again showed a decline in glacial area.

When utilizing area-volume scaling techniques (e.g., Bahr et al., 1997) to determine volume loss based on area change, Bahr et al. (1997) underestimated Dinwoody Glacier's volume loss by approximately 40% for 1983 to 2001 when compared to results utilizing aerial photographs. This difference may be a result of the glaciers, as selected by Bahr et al. (1997), which were distributed throughout the world and may not reflect the extremely steep terrain that is typical of the Wind River Range as noted by Meier (1951). Additionally, the author acknowledges that using one glacier (Dinwoody) to evaluate the area-volume scaling methodology of Bahr et al. (1997) may not be prudent and additional data is needed. Future research should focus on determining area change and volume loss for all 42 glacial complexes in the Wind River Range, utilizing aerial photographs. Thus, area-volume scaling techniques, specific to the Wind River Range, could be developed.

The results also showed that Wind River Range glaciers make appreciable contributions to downstream water flows. Glacial contributions are responsible for approximately 4% to 10% of downstream flows at three different gage stations (using the

Bahr et al., 1997 methods). The downstream flow contributions of glaciers may be underestimated using these methods, since the Bahr et al. (1997) methods significantly underestimated the volume of ice lost from Dinwoody Glacier, thus potentially exacerbating the amount of glacial meltwater contributions to downstream flows.

Interestingly, Marston et al. (1991) estimated the water equivalent lost (using aerial photographs) for Dinwoody Glacier 1958 to 1983 (approximately 25 years) to be 64 $m^3 \times 10^6$. The current study estimated the water equivalent of ice loss (using aerial photographs) for Dinwoody Glacier from 1983 to 2001 (approximately 18 years) to be 60 $m^3 \times 10^6$. Intuitively, one would hypothesize that, as the glacier decreases in size (i.e., less volume), the majority of the glacial mass would become more concentrated at higher elevations, and thus less melting (ice loss) would occur. However, the current research reports an increase in ice loss for a more recent period of record. This result may support Naftz et al. (2002) observations of increased air temperatures recently in the Wind River Range.

6.0 Acknowledgements

This research is supported by the Wyoming Water Development Commission, the Wyoming Water Development Office and the USGS Wyoming Water Research Program. I would like to acknowledge each of my graduate committee members, Glenn Tootle, Greg Kerr, Steven Prager and Ramesh Sivanpillai for their assistance and dedication to this project. Also, recognition is given to Larry Pochop for his expertise throughout this project as well as Fred Ogden for his willingness to assist during the early stages of this project. I would also like to acknowledge Jake Edmunds for assisting with this research, along with Dave Cook and Seth Wittke for technical assistance.

7.0 References

Bahr, D., Meier, M., and Peckman, S., (1997). The physical basis of glacier volume area scaling, *Journal of Geophysical Research*, vol. 102, B9, p. 20,355-20,362.

Braithwaite, R.J., and Olsen, O.B. (1988). Effects of glaciers on annual run-off, Johan Dahl Land, South Greenland. *Journal of Glaciology*, 24, 200-207.

Dyson, J.L., 1952. Glaciers of the American Rocky Mountains. Triennial Report, (1950-52). Committee on Glaciers, American Geophysical Union and American Geographical Society, New York, HY, 37 pp.

Dyurgerov, M.B., and Meier, M.F., (2000). Twentieth century climate change: Evidence from small glaciers, *PNAS*, 97, 1406-1411.

Ferguson, R.I., (1973). Sinuosity of supraglacial streams. *Geological Society of America Bulletin*, 84, 251-255.

Fountain, A.G. (2006). States with Glaciers. Retrieved August 22, 2007 from Portland State University, Glacier Research Website: http://glaciers.research.pdx.edu/states.php

Fountain, A.G., Krimmel, R.M., Trabant, D.C. (1997). Strategy for monitoring glaciers. *US Geological Survey Circular*, 1132, 19.

Fountain, A.G., and Tangborn, W.V. (1985). The effect of glaciers on streamflow variations. *Water Resources Research*, 21, 579-586.

Granshaw, F.D., and Fountain, A.G. (2006). Glacier change (1958-1998) in the North Cascades National Park Complex. Washington USA. *Journal of Glaciology*, 52 (177), 251-256.

Hall, D.K., and Martinec, J. (Ed.). (1985). *Remote sensing of ice and snow*. New York, NY: Chapman and Hall.

Love, C.M. and C.D. Thompson, (1987). Stratigraphy and Recent Melting of Wind River Glaciers, Wyoming. Programme with Abstacts, XII Congress of International Union for Quaternary Research, Ottawa, Canada, p. 215.

Love, C.M. and C.D. Thompson, (1988). Reconnaissance Survey; Trace Metals Concentration in Wind River Glaciers. Technical Report prepared for Wyoming water Research Center, Laramie, WY, 78 pp.

Maidment, D.R. (Ed.). (1993). *Handbook of Hydrology*. McGraw-Hill, Inc. New York, NY: Mcgraw Hill Inc.

Marston, R.A., Pochop, L.O., Kerr, G.L., Varuska M.L., and Veryzer, D.J., (1991). Recent glacier changes in the Wind River Range, Wyoming. *Physical Geography*, 12, 2, 115-123.

Mears, B., Jr., (1972). Wyoming's Glaciers, Past and Present. Wyoming Wildlife 36:26-34.

Meier, M.F., (1951). *Glaciers of the Gannett Peak-Fremont Peak area, Wyoming*. M.S. Thesis. The State University of Iowa.

Meier, M.F. (1969). Glaciers and water supply. *American Water Works Association*, 81, 8-12.

Meier, M.F. (1973). Evaluation of ERTS imagery for mapping and detection of changes in snowcover on land and on glaciers, *Symposium on Significant Results Obtained from the earth resources Technology Satellite-1, National Aeronautics and Space Administration*, Washington DC, 1, 863-875.

Meier, M.F., and Post, A.S. (1962). Recent variations in mass net budgets of glaciers in western North America. *Symposium of Obergurgl*, 63-77.

Naftz, David L., D.D. Susong, P.F. Schuster, L.D. Cecil, M.D. Dettinger, R.L. Michel, and C. Kendall, (2002). Ice core evidence of rapid air temperature increases since 1960 in alpine areas of the Wind River Range, Wyoming, United States. Journal of Geophysical Research (Atmospheres), Volume 107, Issue D13, pp. ACL 3-1, CiteID 4171, DOI 10.1029/2001JD000621

Navidi, William (Ed.). (2006). *Statistics for Engineers and Scientists*. McGraw-Hill, Inc. New York, NY: Mcgraw Hill Inc.

Osterkamp, W.R., and Parker, R.S. (1991). Sediment monitoring in the United States, in Fan, S., and Kuo, Y., eds., Proceedings*: Federal Interagency Sedimentation Cenference, 5th*, 1991, Las Vegas, 115-129.

Pochop, L.O., Marston, R.A., Kerr, G.L., Veryzer, D.J., and Jacobel, R. (1990). Glacial icemelt in the Wind River Range, Wyoming. In *Watershed Planning and Analysis in Action*. Durango, CO: American Society of Civil Engineers, 118-124.

Wilkerson, F.D., and Schmid, G.L. (2003). Debris flow in Glacier National Park, Montana: geomorphology and hazards. *Geomorphology*, 55, 317-328.

Wolken, G.J. (2000). *Energy balance and spatial distribution of net radiation on Dinwoody Glacier, Wind River Range, Wyoming, USA*. M.S. Thesis, Dept. of Geography and Recreation, University of Wyoming.

8.0 Appendices

8.1 Appendix 1: Personnel and Equipment / Supplies used for 2006 Fieldwork

Name	Status	Area
Kyle Cheesbrough	Graduate student	Civil and Architectural Engineering
Anthony Barnett	Graduate student	Civil and Architectural Engineering
John Bellamy	Graduate student	Civil and Architectural Engineering
Tim Tschetter	Graduate student	Geology
Greg Kerr	Academic Professional	Civil and Architectural Engineering
Glenn Tootle	Assistant Professor	Civil and Architectural Engineering

Equipment	Supplies
2 Trimble ProXRS GPS units	Access permits
10 Trimble battery packs	Bear proof canisters
3 handheld Garmin Vista Cx GPS units	Outdoor recreation gear
Ice radar unit	Food
Ice core auger	First aid kits
Sample bottles for isotope analysis	
Digital cameras	
Hand held radios	
Satellite phone	

8.2 Appendix 2: Locations of GPS Point Measurments

UTM WGS 1984 Zone 12N

EASTING	NORTHING	GPS_HEIGHT	GPS_DATE		EASTING	NORTHING	GPS_HEIGHT	GPS_DATE
610466.6	4781413.2	3472.1	8/9/2006		610277.1	4781201.3	3518.9	8/9/2006
610460.5	4781396.8	3475.5	8/9/2006		610295.9	4781255.9	3511.3	8/9/2006
610438.0	4781380.3	3481.9	8/9/2006		610315.8	4781301.1	3505.2	8/9/2006
610403.3	4781362.8	3489.5	8/9/2006		610455.7	4781389.7	3476.7	8/9/2006
610356.6	4781336.1	3497.9	8/9/2006		610455.5	4781388.7	3477.4	8/9/2006
610301.9	4781321.5	3508.8	8/9/2006		610452.9	4781348.3	3481.2	8/9/2006
610237.6	4781301.0	3522.1	8/9/2006		610437.4	4781256.2	3489.6	8/9/2006
610237.2	4781204.1	3529.1	8/9/2006		610410.1	4781212.4	3496.4	8/9/2006
610219.5	4781158.1	3539.7	8/9/2006		610413.3	4781179.2	3499.3	8/9/2006
610240.3	4781134.3	3534.7	8/9/2006		610427.7	4781072.2	3510.0	8/9/2006
610187.9	4781108.8	3555.4	8/9/2006		610478.1	4781017.0	3512.7	8/9/2006
610144.9	4781093.1	3570.0	8/9/2006		610493.3	4780988.7	3515.3	8/9/2006
610165.3	4781042.0	3566.8	8/9/2006		610469.4	4781393.5	3473.9	8/10/2006
610235.2	4780966.2	3554.2	8/9/2006		610504.0	4781358.9	3470.0	8/10/2006
610277.1	4780929.9	3547.7	8/9/2006		610545.0	4781291.3	3470.0	8/10/2006
610311.7	4780867.3	3557.4	8/9/2006		610576.0	4781202.4	3475.2	8/10/2006
610334.4	4780806.1	3575.4	8/9/2006		610627.8	4781220.0	3465.2	8/10/2006
610375.0	4780764.7	3586.9	8/9/2006		610689.1	4781240.1	3454.8	8/10/2006
610400.1	4780749.2	3591.1	8/9/2006		610764.8	4781187.4	3459.8	8/10/2006
610437.2	4780771.2	3581.3	8/9/2006		610831.8	4781187.5	3463.4	8/10/2006
610467.3	4780830.4	3557.8	8/9/2006		610881.2	4781215.2	3462.0	8/10/2006
610476.1	4780859.6	3547.0	8/9/2006		610936.3	4781300.4	3449.9	8/10/2006
610482.3	4780882.0	3539.9	8/9/2006		611007.7	4781308.1	3451.3	8/10/2006
610518.6	4780876.7	3535.7	8/9/2006		611084.9	4781318.2	3448.7	8/10/2006
610560.2	4780854.8	3537.9	8/9/2006		611120.5	4781262.9	3465.0	8/10/2006
610622.5	4780840.8	3539.2	8/9/2006		611165.0	4781186.1	3486.2	8/10/2006
610667.8	4780819.6	3546.3	8/9/2006		611210.2	4781120.4	3499.7	8/10/2006
610710.9	4780783.3	3551.2	8/9/2006		611251.7	4781064.9	3507.8	8/10/2006
610721.2	4780767.5	3555.3	8/9/2006		611298.1	4781000.3	3515.4	8/10/2006
610776.0	4780747.1	3551.8	8/9/2006		611369.5	4780937.6	3524.4	8/10/2006
610815.8	4780728.8	3552.1	8/9/2006		611439.0	4780872.8	3539.0	8/10/2006
610861.6	4780696.5	3557.1	8/9/2006		611491.5	4780841.7	3551.3	8/10/2006
610923.1	4780655.7	3561.5	8/9/2006		611540.5	4780806.4	3567.2	8/10/2006
610987.2	4780613.9	3565.3	8/9/2006		611604.5	4780785.3	3582.5	8/10/2006
611037.4	4780609.1	3565.9	8/9/2006		611655.5	4780831.9	3589.0	8/10/2006
610998.5	4780658.4	3555.1	8/9/2006		611691.1	4780762.1	3605.4	8/10/2006
610961.5	4780683.1	3550.8	8/9/2006		611743.9	4780660.2	3630.7	8/10/2006
610911.7	4780711.7	3547.7	8/9/2006		611776.7	4780581.5	3650.1	8/10/2006
610873.1	4780748.1	3541.9	8/9/2006		611789.0	4780526.3	3666.7	8/10/2006
610825.5	4780777.9	3538.8	8/9/2006		611753.8	4780578.7	3649.2	8/10/2006
610765.5	4780803.0	3537.0	8/9/2006		611705.8	4780597.1	3633.1	8/10/2006
610720.0	4780834.8	3531.3	8/9/2006		611664.5	4780597.3	3624.1	8/10/2006
610650.4	4780872.9	3526.2	8/9/2006		611608.4	4780542.5	3625.8	8/10/2006

610617.4	4780882.7	3525.7	8/9/2006		611549.2	4780491.6	3624.1	8/10/2006
610572.1	4780910.6	3520.5	8/9/2006		611494.7	4780481.9	3617.4	8/10/2006
610517.4	4780928.2	3524.0	8/9/2006		611468.1	4780477.0	3614.8	8/10/2006
610458.8	4780943.8	3526.6	8/9/2006		611489.2	4780515.8	3604.8	8/10/2006
610412.1	4780943.6	3529.6	8/9/2006		611492.7	4780565.8	3592.3	8/10/2006
610367.2	4780951.1	3531.0	8/9/2006		611470.6	4780630.6	3576.7	8/10/2006
610319.3	4780968.5	3533.8	8/9/2006		611428.1	4780677.4	3563.8	8/10/2006
610279.2	4781003.7	3535.8	8/9/2006		611369.4	4780655.2	3570.1	8/10/2006
610255.1	4781032.8	3539.3	8/9/2006		611399.1	4780748.3	3549.1	8/10/2006
610252.4	4781063.1	3537.6	8/9/2006		611374.5	4780815.0	3537.8	8/10/2006
610252.9	4781107.5	3534.0	8/9/2006		611296.3	4780842.6	3541.0	8/10/2006
610266.1	4781149.6	3526.6	8/9/2006		611240.4	4780849.4	3541.9	8/10/2006

8.3 Appendix 3: Locations of Radar Depth Measurments

UTM WGS 1984 Zone 12N

Point #	X (m)	Y (m)	Elevation (m)	Ice Depth (m)		Point #	X (m)	Y (m)	Elevation (m)	Ice Depth (m)
1	610517	4781212	3474	36.58		72	610781	4780663	3534	38.14
2	610365	4781124	3524	35.16		73	610784	4780664	3535	37.37
3	610375	4781087	3523	35.73		74	610790	4780668	3535	37.39
4	610359	4781083	3523	34.88		75	610803	4780659	3538	37.44
5	610358	4781085	3525	34.60		76	610812	4780657	3539	37.70
6	610360	4781096	3524	33.06		77	610813	4780656	3540	37.39
7	610363	4781099	3526	32.00		78	610826	4780654	3538	36.81
8	610361	4781086	3525	31.31		79	610840	4780653	3538	35.96
9	610365	4781078	3525	31.22		80	610855	4780647	3541	35.26
10	610371	4781074	3523	31.56		81	610863	4780642	3540	34.83
11	610369	4781078	3525	31.79		82	610882	4780643	3543	34.38
12	610366	4781074	3526	32.24		83	610887	4780644	3543	33.92
13	610368	4781073	3525	33.04		84	610888	4780645	3543	33.49
14	610368	4781056	3524	34.06		85	610906	4780635	3544	33.07
15	610367	4781054	3526	35.79		86	610921	4780628	3544	33.00
16	610367	4781025	3526	37.29		87	610928	4780623	3545	33.10
17	610366	4781038	3527	38.02		88	610944	4780626	3548	33.21
18	610365	4781035	3526	39.58		89	610948	4780624	3549	33.74
19	610363	4781032	3527	43.44		90	610961	4780616	3550	35.94
20	610357	4781029	3528	46.07		91	610972	4780614	3551	40.66
21	610359	4781028	3526	48.39		92	610994	4780609	3549	46.35
22	610359	4781020	3526	50.72		93	610994	4780609	3549	51.29
23	610366	4781015	3526	52.42		94	611017	4780604	3552	55.24
24	610363	4781013	3525	53.81		95	611030	4780603	3551	58.39
25	610358	4781018	3527	54.57		96	611044	4780617	3552	60.31
26	610358	4781017	3527	55.19		97	611049	4780603	3555	62.23
27	610362	4781006	3531	55.31		98	611060	4780599	3556	64.14
28	610359	4781012	3528	54.85		99	611129	4781384	3554	65.28
29	610354	4780995	3527	54.46		100	611128	4781360	3553	66.38
30	610350	4780990	3527	53.68		101	611099	4780600	3554	67.48
31	610351	4780989	3526	53.27		102	611109	4780605	3557	69.09
32	610351	4781002	3527	54.29		103	611127	4780589	3557	70.97
33	610356	4780996	3527	53.78		104	611136	4780597	3557	73.68
34	610359	4780956	3528	51.45		105	611165	4780602	3557	76.42
35	610358	4780958	3529	50.21		106	611175	4780604	3557	79.28
36	610359	4780958	3528	49.13		107	611195	4780585	3556	81.76
37	610358	4780958	3527	48.34		108	611196	4780593	3557	84.14
38	610360	4780960	3527	47.92		109	611217	4780608	3560	86.33
39	610362	4780961	3527	47.54		110	611220	4780605	3560	87.93
40	610376	4780956	3527	47.48		111	611231	4780602	3561	89.53
41	610377	4780954	3527	47.40		112	611245	4780610	3562	91.70
42	610375	4780950	3527	47.40		113	611257	4780603	3563	93.95

43	610374	4780946	3527	48.04		114	611265	4780605	3562	94.99
44	610443	4781049	3527	49.42		115	611276	4780611	3563	95.51
45	610401	4780940	3528	49.59		116	611288	4780604	3563	96.25
46	610394	4780931	3528	49.82		117	611300	4780604	3565	97.20
47	610392	4780931	3528	48.91		118	611316	4780598	3565	97.58
48	610392	4780930	3528	48.86		119	611315	4780600	3565	97.46
49	610391	4780929	3529	48.46		120	611337	4780601	3563	97.35
50	610444	4781056	3529	47.78		121	611350	4780603	3564	97.24
51	610393	4780920	3531	47.50		122	611359	4780596	3564	97.17
52	610379	4780944	3534	47.17		123	611370	4780600	3565	97.10
53	610371	4780959	3537	46.54		124	611383	4780595	3564	97.76
54	610375	4780955	3538	45.90		125	611397	4780593	3564	98.70
55	610355	4781002	3537	44.97		126	611415	4780594	3563	100.10
56	610358	4781038	3533	44.72		127	611427	4780592	3561	100.66
57	610363	4781089	3530	44.80		128	611434	4780592	3557	100.66
58	610353	4781127	3526	44.16		129	611446	4780590	3557	100.66
59	610374	4780803	3526	42.16		130	611471	4780592	3558	100.46
60	610456	4780837	3527	41.48		131	611476	4780595	3560	100.23
61	610459	4780808	3529	40.77		132	611484	4780598	3561	99.11
62	610503	4780770	3534	40.38		133	611502	4780595	3563	96.80
63	610537	4780745	3538	40.43		134	611502	4780592	3566	94.63
64	610577	4780713	3542	40.94		135	611510	4780596	3568	91.96
65	610616	4780673	3545	41.47		136	611525	4780596	3570	88.74
66	610632	4780659	3546	41.34		137	611523	4780598	3570	85.71
67	610686	4780657	3543	40.98		138	611532	4780603	3572	82.78
68	610723	4780653	3541	40.45		139	611553	4780608	3572	78.84
69	610732	4780671	3533	39.77		140	611562	4780613	3572	75.08
70	610744	4780669	3534	39.65		141	611574	4780615	3573	72.38
71	610764	4780670	3534	39.47						

8.4 Appendix 4: Comparison of GPS & Stereo Model Elevations

UTM WGS 1984 Zone 12N			
EASTING	NORTHING	GPS ELEVATION (m)	STEREO MODEL ELEVATION (m)
610466.57	4781413.21	3472.15	3462.37
610460.45	4781396.80	3475.54	3467.98
610437.97	4781380.32	3481.88	3471.26
610403.30	4781362.80	3489.48	3476.95
610356.57	4781336.06	3497.87	3481.48
610301.93	4781321.48	3508.78	3502.16
610237.63	4781301.01	3522.09	3512.47
610237.15	4781204.09	3529.06	3521.58
610219.52	4781158.14	3539.74	3531.02
610240.34	4781134.27	3534.67	3540.89
610187.90	4781108.78	3555.45	3546.22
610144.92	4781093.12	3569.96	3547.26
610165.35	4781042.01	3566.77	3559.76
610235.19	4780966.16	3554.18	3558.86
610277.05	4780929.94	3547.66	3542.09
610311.74	4780867.32	3557.40	3553.15
610334.37	4780806.10	3575.38	3568.02
610374.96	4780764.73	3586.89	3572.01
610400.11	4780749.18	3591.06	3576.80
610437.24	4780771.23	3581.31	3585.50
610467.28	4780830.36	3557.79	3547.12
610476.12	4780859.65	3547.02	3542.20
610482.25	4780882.03	3539.90	3536.09
610518.63	4780876.73	3535.68	3535.78
610560.24	4780854.85	3537.88	3527.08
610622.49	4780840.75	3539.19	3536.99
610667.76	4780819.57	3546.29	3539.23
610710.89	4780783.28	3551.20	3547.65
610721.21	4780767.47	3555.35	3547.82
610775.95	4780747.14	3551.83	3552.62
610815.79	4780728.80	3552.12	3550.77
610861.61	4780696.50	3557.13	3543.28
610923.15	4780655.75	3561.47	3548.71
610987.16	4780613.88	3565.26	3553.21
611037.38	4780609.08	3565.94	3556.89
610998.49	4780658.43	3555.09	3549.54
610961.51	4780683.07	3550.84	3547.74
610911.73	4780711.71	3547.69	3540.18
610873.12	4780748.10	3541.91	3538.46
610825.46	4780777.88	3538.83	3530.17
610765.52	4780803.03	3537.03	3529.64
610720.04	4780834.83	3531.30	3525.45
610650.44	4780872.94	3526.24	3520.79

610617.41	4780882.67	3525.74	3520.14
610572.11	4780910.63	3520.49	3519.56
610517.38	4780928.24	3524.01	3518.73
610458.81	4780943.83	3526.56	3520.14
610412.05	4780943.60	3529.65	3520.65
610367.23	4780951.07	3530.99	3522.16
610319.25	4780968.55	3533.82	3525.47
610279.16	4781003.69	3535.85	3530.21
610255.11	4781032.85	3539.28	3533.97
610252.44	4781063.15	3537.56	3534.58
610252.85	4781107.46	3533.96	3528.46
610266.14	4781149.59	3526.60	3520.14
610277.12	4781201.27	3518.87	3515.46
610295.92	4781255.85	3511.30	3502.31
610315.75	4781301.10	3505.21	3498.25
610455.68	4781389.67	3476.74	3581.46
610455.51	4781388.75	3477.35	3475.98
610452.85	4781348.32	3481.18	3470.15
610437.43	4781256.19	3489.55	3478.81
610410.12	4781212.42	3496.41	3491.23
610413.25	4781179.25	3499.27	3492.67
610427.67	4781072.18	3509.95	3500.90
610478.13	4781016.99	3512.68	3508.49
610493.28	4780988.65	3515.34	3510.97
610469.38	4781393.53	3473.87	3470.10
610503.98	4781358.90	3470.04	3465.12
610544.96	4781291.31	3469.95	3461.01
610576.03	4781202.39	3475.20	3470.16
610627.78	4781219.96	3465.22	3464.54
610689.10	4781240.06	3454.76	3452.89
610764.82	4781187.43	3459.75	3456.90
610831.75	4781187.48	3463.42	3461.10
610881.18	4781215.16	3461.97	3455.12
610936.33	4781300.37	3449.94	3445.69
611007.71	4781308.12	3451.27	3450.16
611084.87	4781318.16	3448.74	3443.17
611120.47	4781262.90	3465.03	3462.13
611164.98	4781186.08	3486.19	3480.20
611210.16	4781120.40	3499.72	3488.26
611251.70	4781064.90	3507.81	3500.68
611298.11	4781000.34	3515.35	3510.24
611369.48	4780937.61	3524.37	2517.26
611439.04	4780872.81	3539.04	3535.64
611491.51	4780841.70	3551.31	3548.71
611540.46	4780806.39	3567.22	3562.16
611604.50	4780785.35	3582.46	3580.16
611655.47	4780831.93	3588.99	3582.69

611691.09	4780762.10	3605.45	3601.23
611743.92	4780660.22	3630.73	3620.75
611776.68	4780581.52	3650.12	3643.78
611789.02	4780526.34	3666.68	3658.21
611753.77	4780578.68	3649.19	3642.89
611705.85	4780597.12	3633.06	3630.78
611664.50	4780597.28	3624.13	3622.56
611608.42	4780542.55	3625.80	3620.47
611549.22	4780491.60	3624.12	3620.68
611494.70	4780481.90	3617.36	3612.47
611468.05	4780476.97	3614.82	3613.87
611489.20	4780515.80	3604.75	3598.46
611492.73	4780565.82	3592.30	3590.47
611470.55	4780630.60	3576.73	3578.68
611428.14	4780677.42	3563.80	3560.47
611369.45	4780655.20	3570.15	3568.46
611399.14	4780748.33	3549.10	3438.64
611374.52	4780815.00	3537.76	3526.71
611296.35	4780842.56	3541.04	3530.78
611240.44	4780849.39	3541.94	3536.19